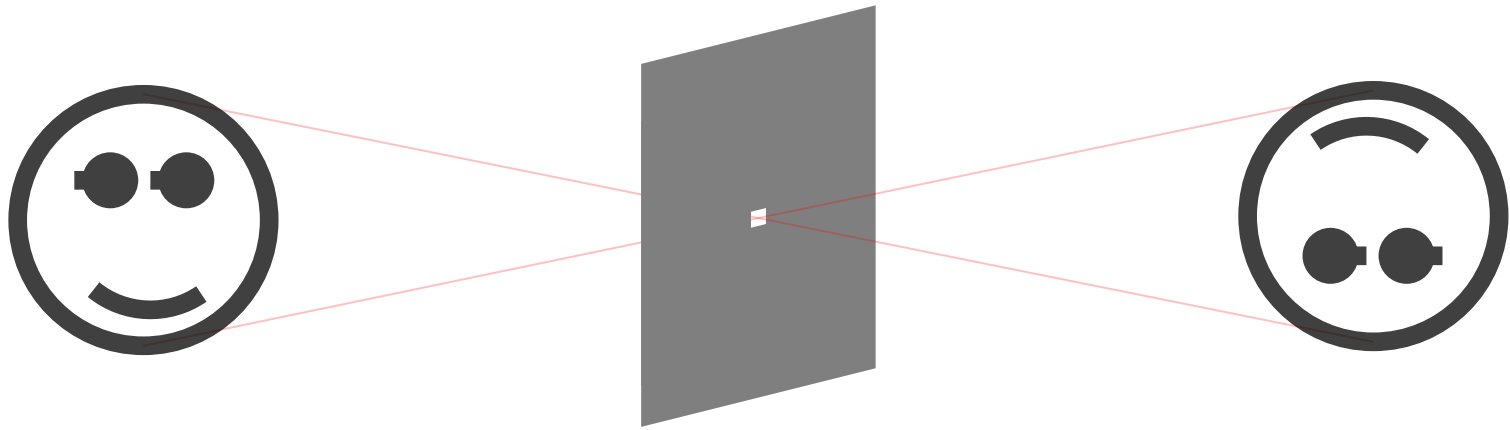


Measurements of Small Vertical Beamsizes using a Coded Aperture at Diamond Light Source

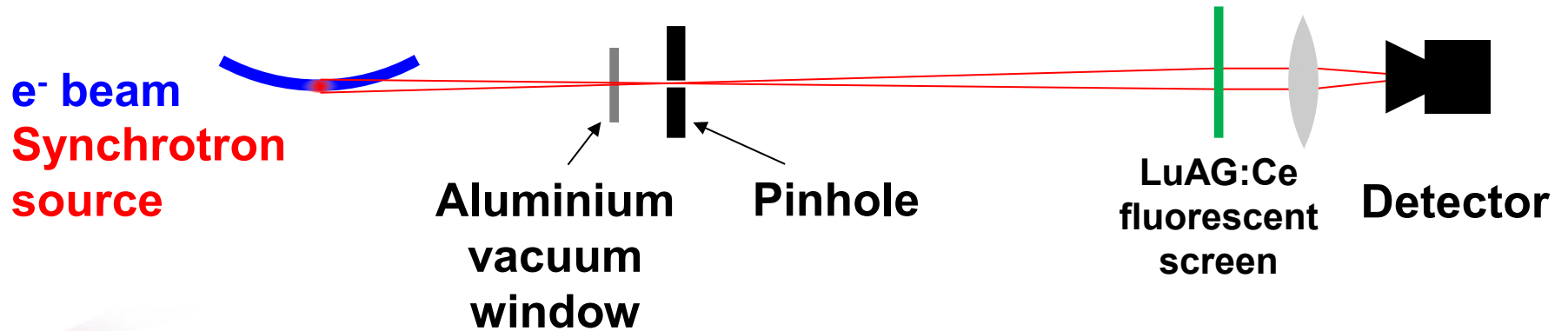
C. Bloomer
G. Rehm
J.W. Flanagan

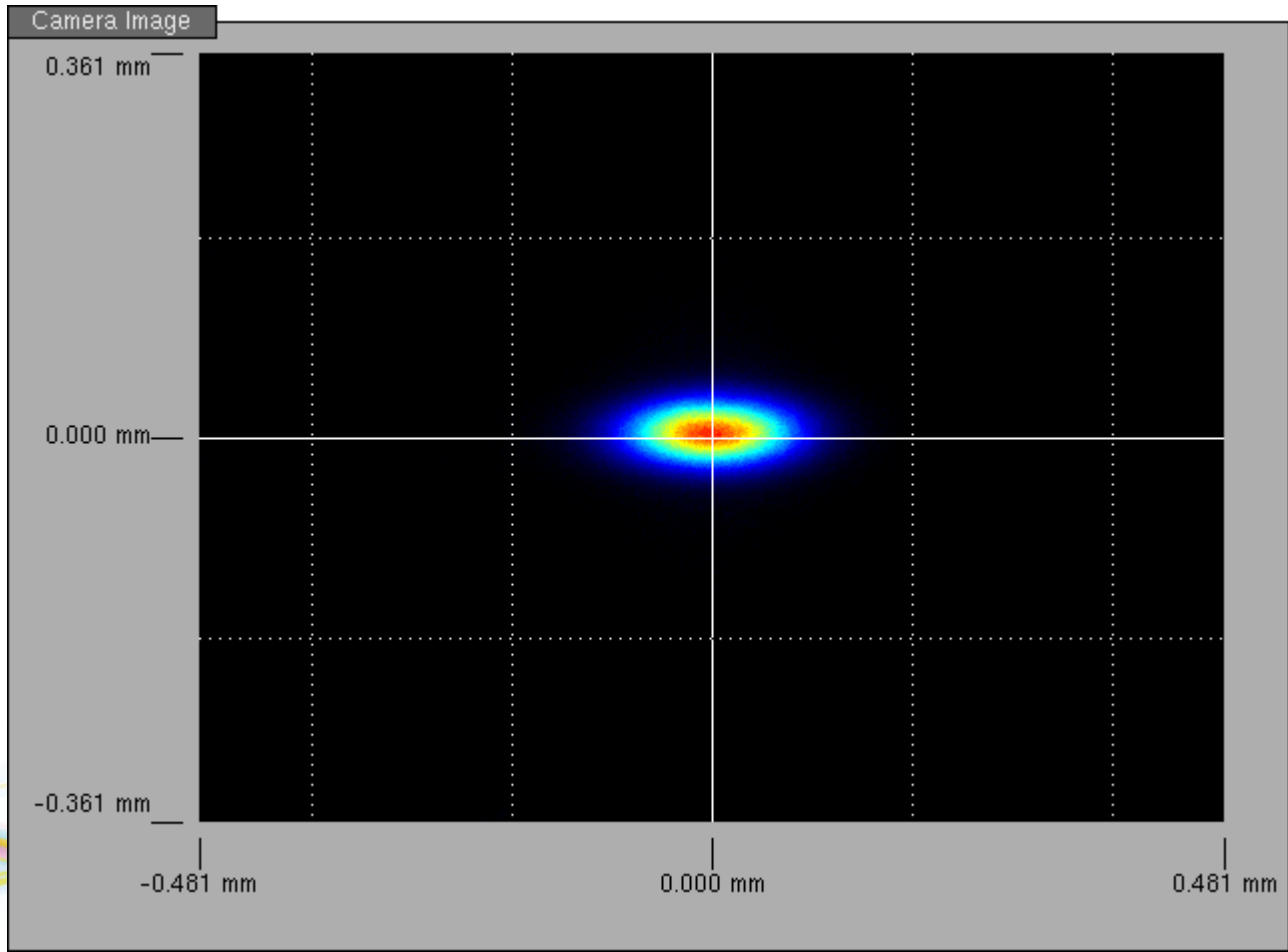


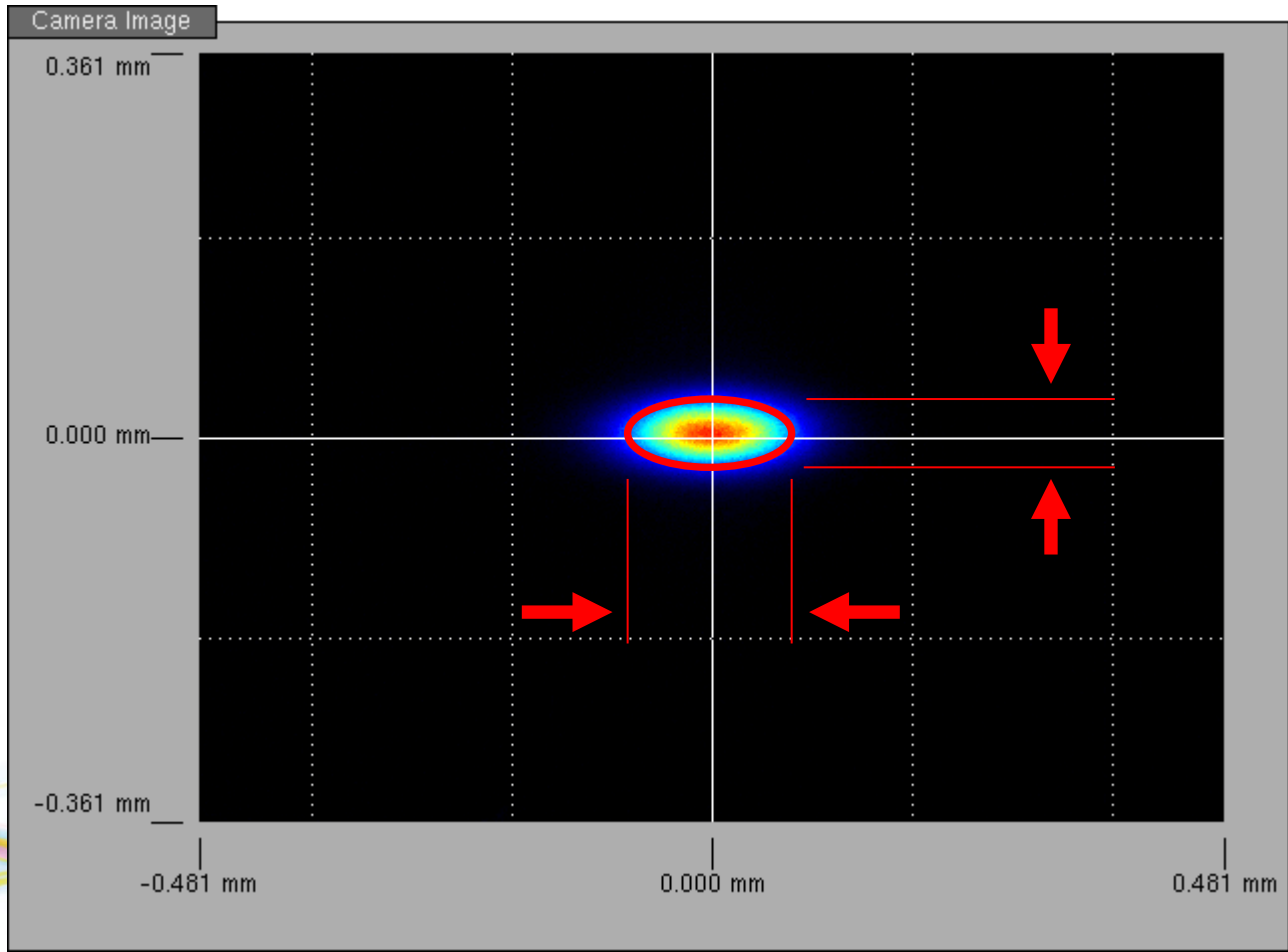
Pinhole camera



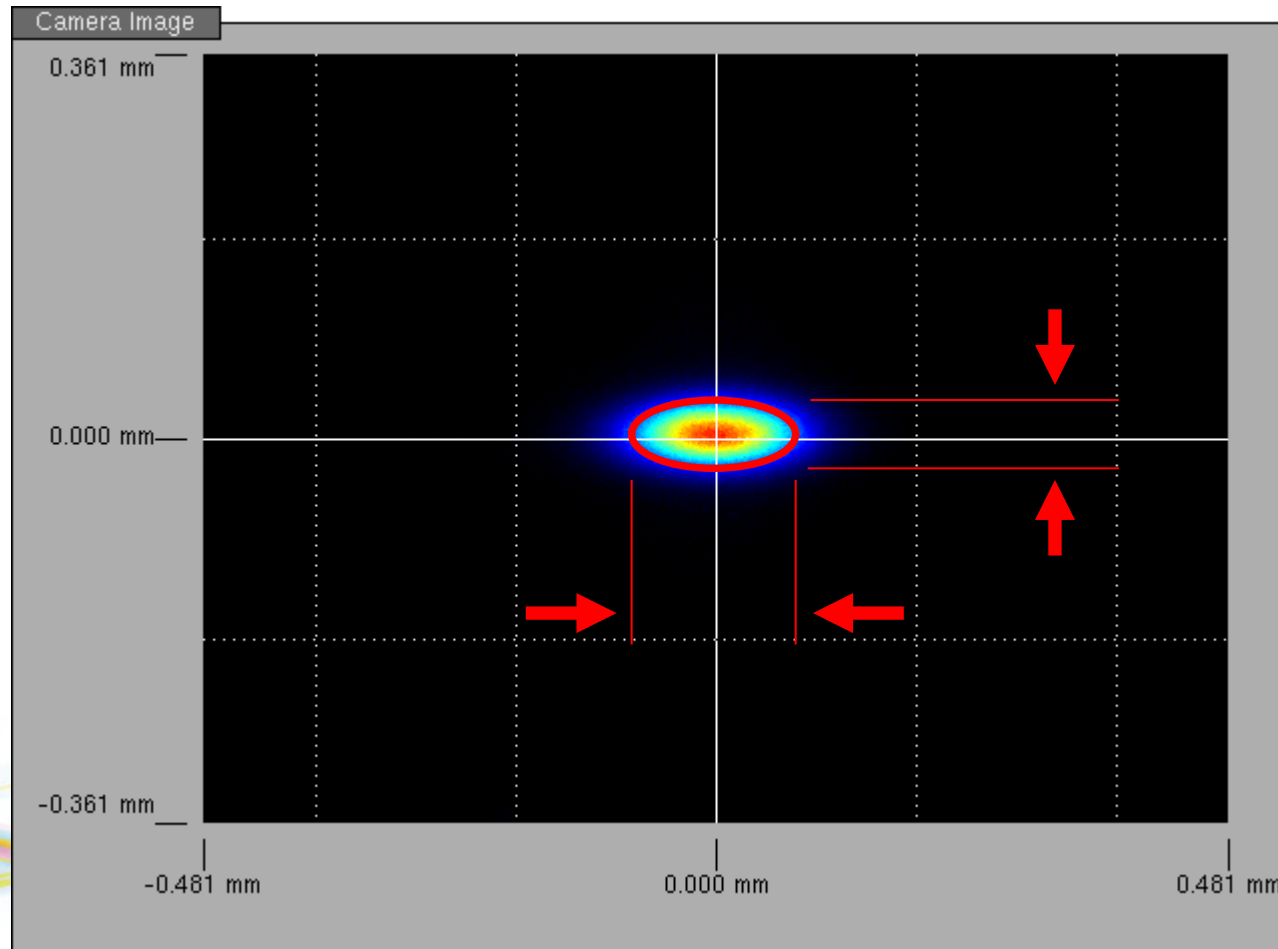
Pinhole camera



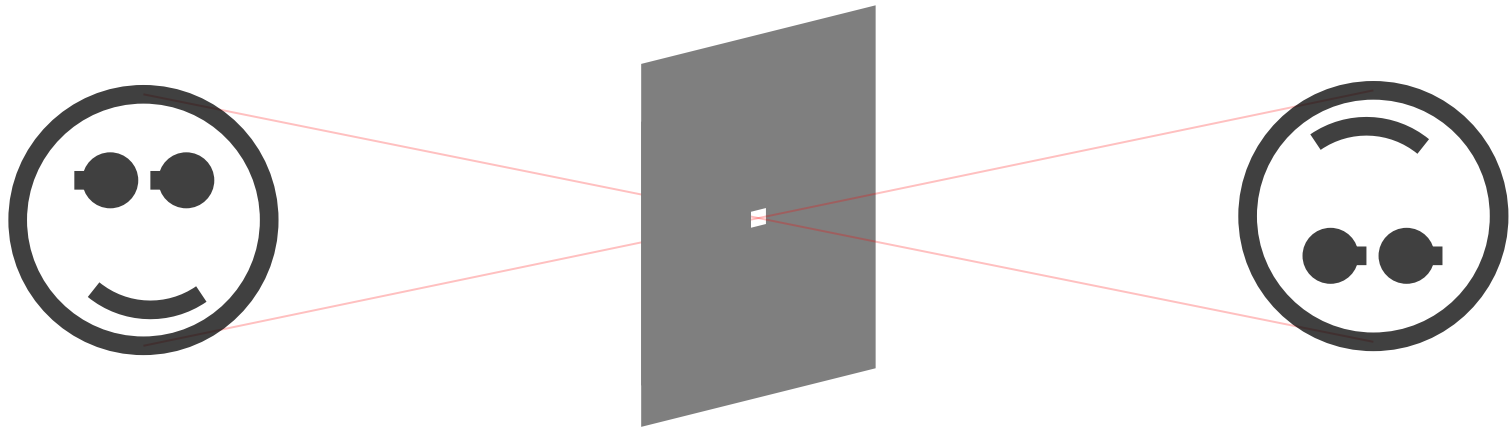




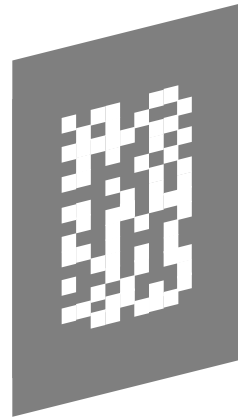
Beam size calculated from Gaussian fit



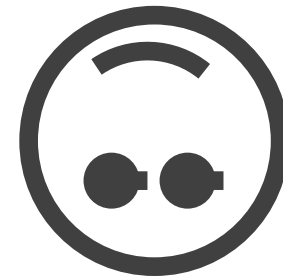
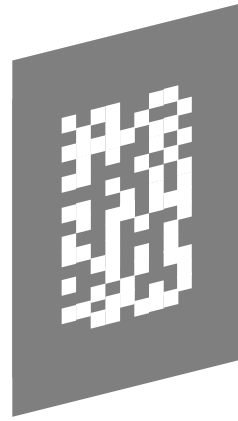
Pinhole camera



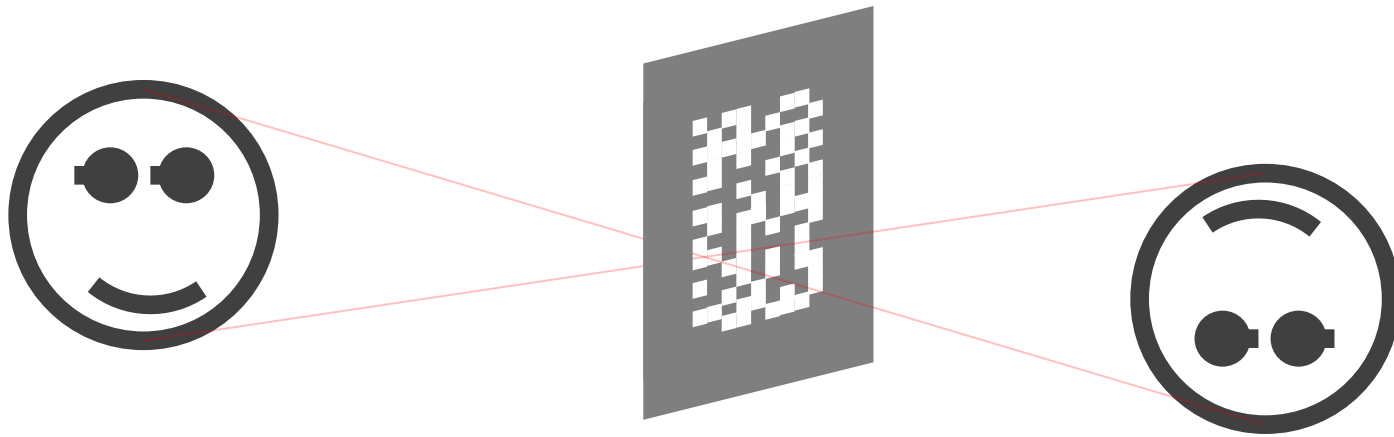
Coded aperture



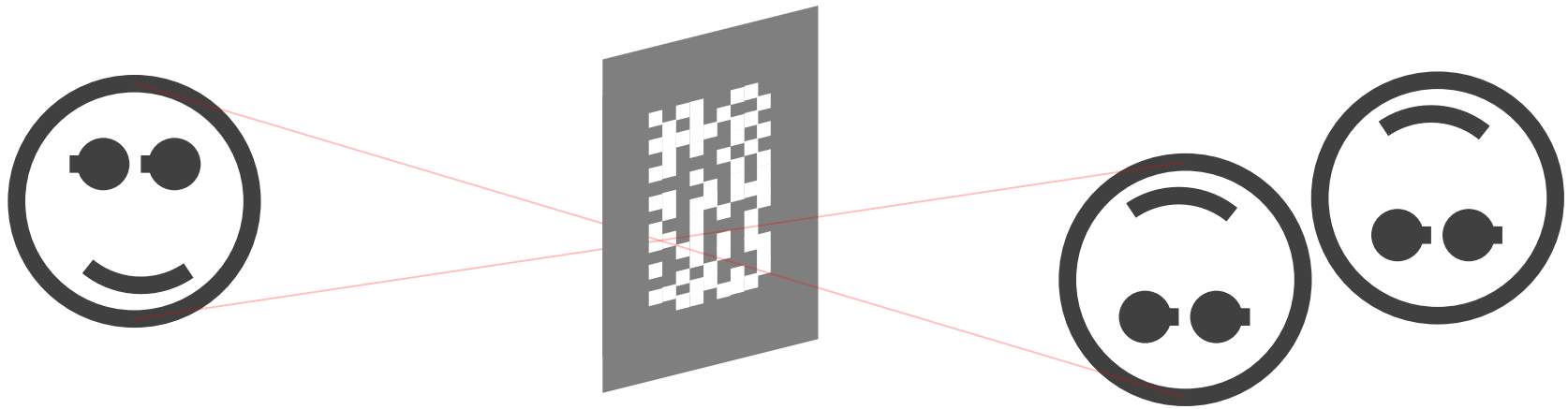
Coded aperture



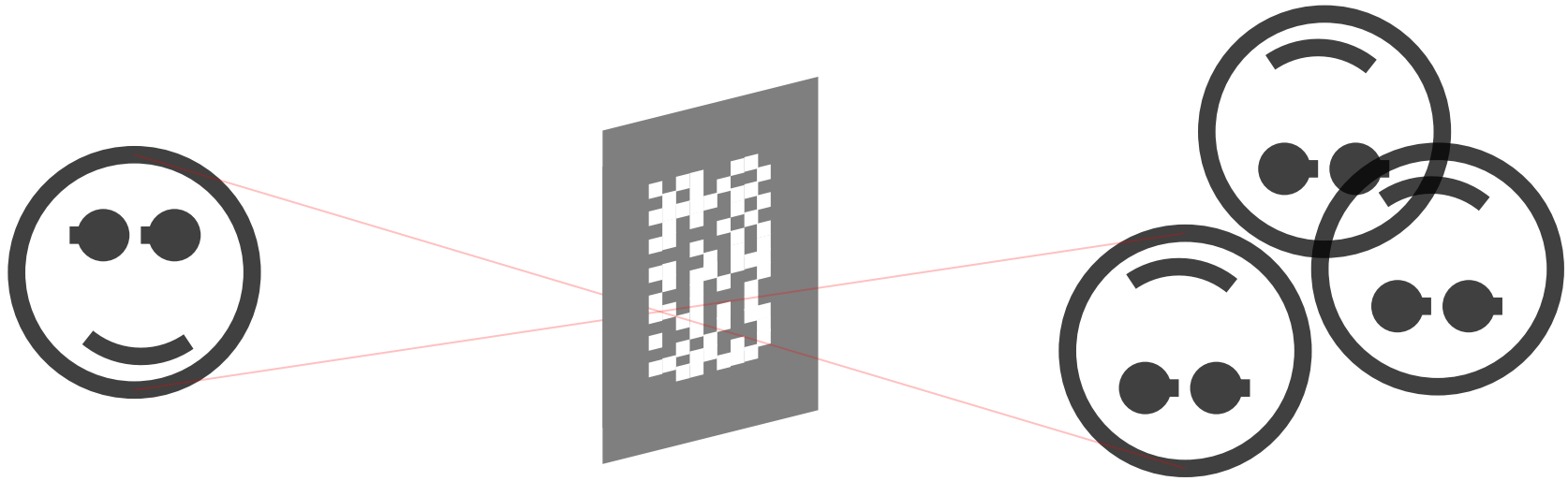
Coded aperture



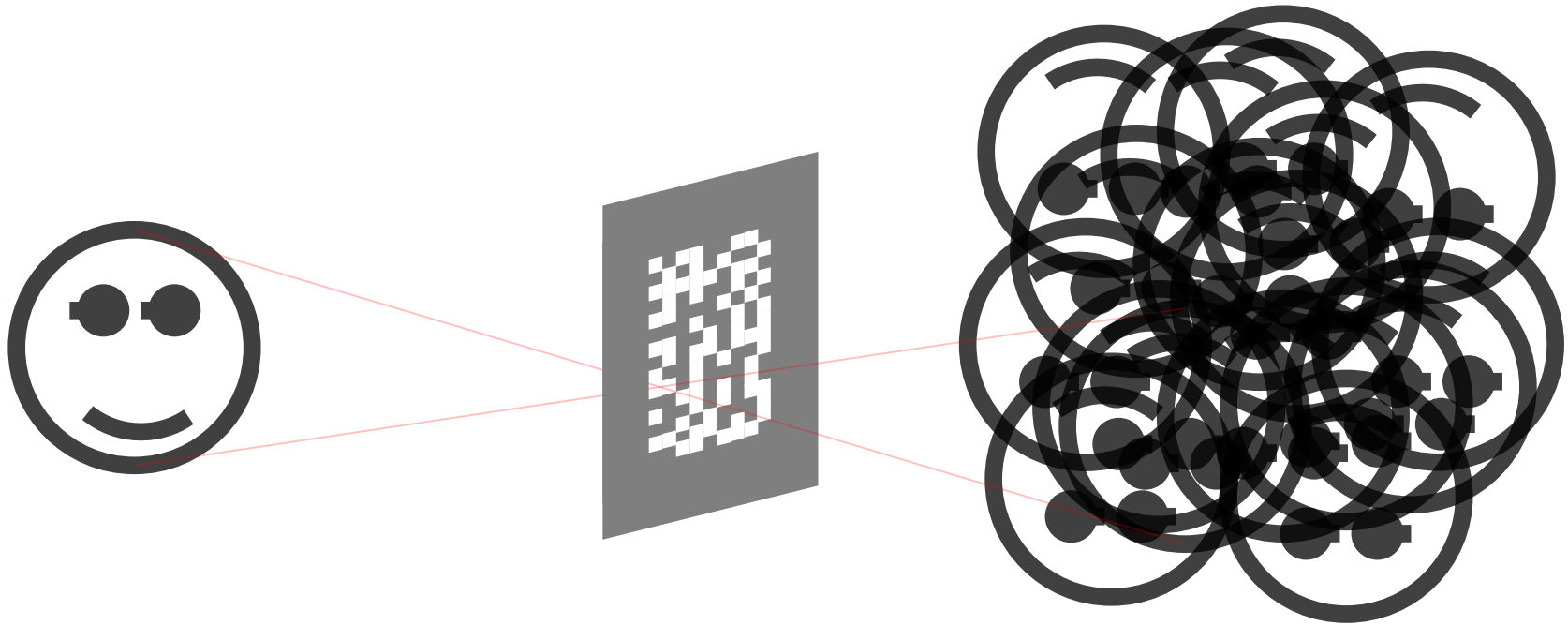
Coded aperture



Coded aperture



Coded aperture



SCATTER-HOLE CAMERAS FOR X-RAYS AND GAMMA RAYS*

R. H. DICKE

Palmer Physical Laboratory, Princeton University

Received June 11, 1968

ABSTRACT

A pinhole camera for which the entrance area, covered with a very large number of randomly distributed pinholes, is 50 per cent open is shown to be a very effective way of forming images of a complex of X-ray stars. A simple statistical trick is used to reduce the multitudinous overlapping images to a single image. Less than forty detected photons are needed to form an image of a single star.

SCATTER-HOLE CAMERAS FOR X-RAYS AND GAMMA RAYS*

R. H. DICKE

Palmer Physical Laboratory, Princeton University

Received June 11, 1968

ABSTRACT

A pinhole camera for which the entrance area, covered with a very large number of randomly distributed pinholes, is 50 per cent open is shown to be a very effective way of forming images of a complex of X-ray stars. A simple statistical trick is used to reduce the multitudinous overlapping images to a single image. Less than forty detected photons are needed to form an image of a single star.

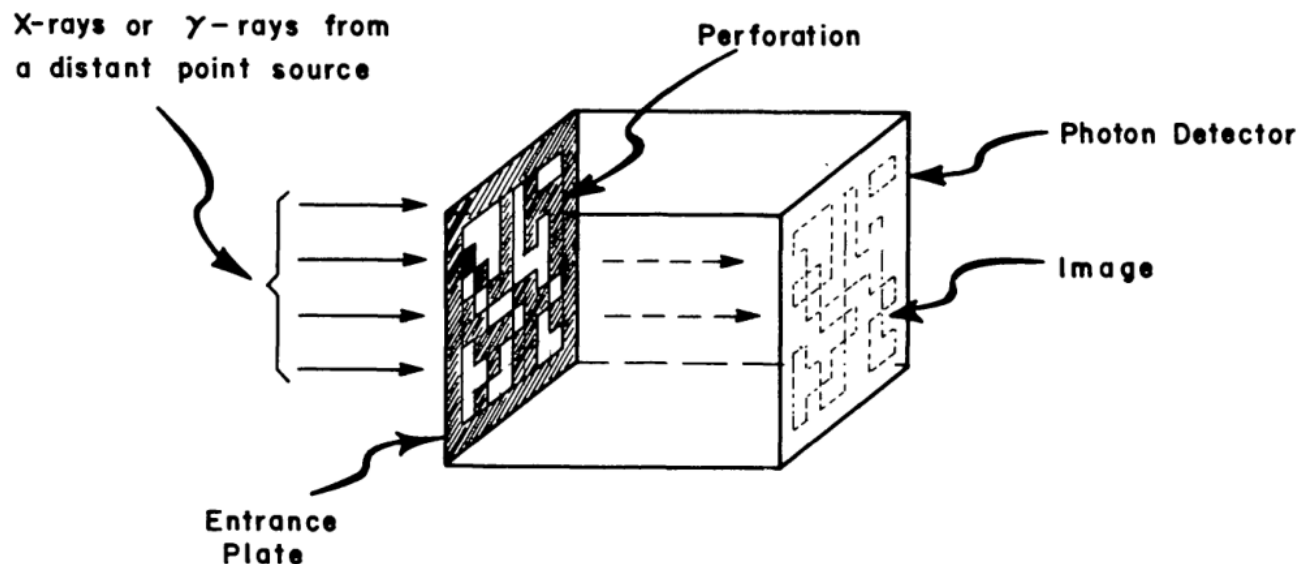


FIG. 1.—Scatter-hole camera. The entrance plate is randomly perforated to provide randomly positioned pinholes. The image is recorded photographically, photoelectrically, or with a photon counter, such as a wire spark chamber.

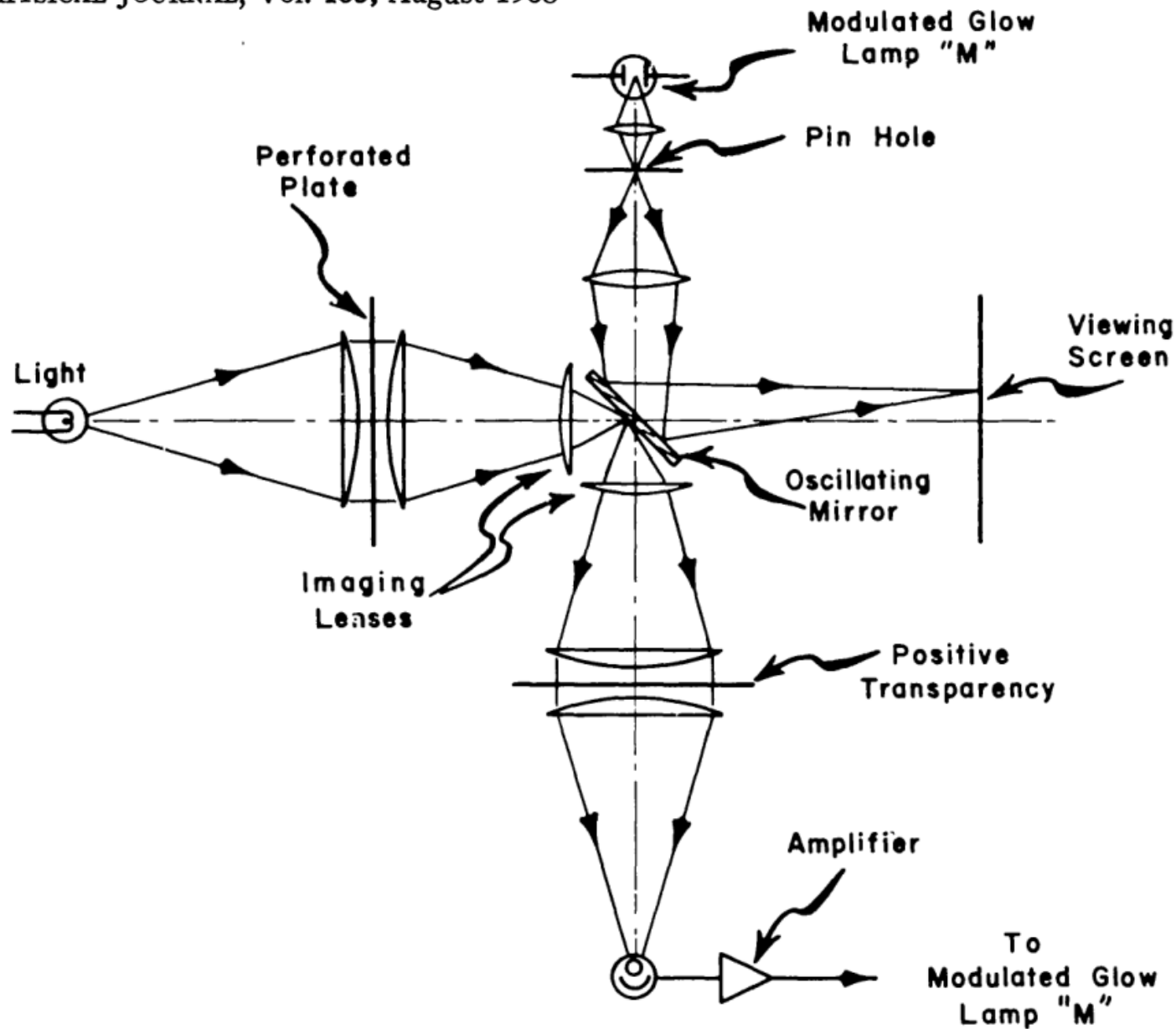


FIG. 2.—The oscillating mirror is double-sided. It provides a scanning of the image position by the entrance pattern and simultaneously a read-out of the rectified image.

Coded aperture imaging with uniformly redundant arrays

E. E. Fenimore and T. M. Cannon

Uniformly redundant arrays (URA) have autocorrelation functions with perfectly flat sidelobes. The URA combines the high-transmission characteristics of the random array with the flat sidelobe advantage of the nonredundant pinhole arrays. This gives the URA the capability to image low-intensity, low-contrast sources. Furthermore, whereas the inherent noise in random array imaging puts a limit on the obtainable SNR, the URA has no such limit. Computer simulations show that the URA with significant shot and background noise is vastly superior to random array techniques without noise. Implementation permits a detector which is smaller than its random array counterpart.

Coded aperture imaging with uniformly redundant arrays

E. E. Fenimore and T. M. Cannon

Uniformly redundant arrays (URA) have autocorrelation functions with perfectly flat sidelobes. The URA combines the high-transmission characteristics of the random array with the flat sidelobe advantage of the nonredundant pinhole arrays. This gives the URA the capability to image low-intensity, low-contrast sources. Furthermore, whereas the inherent noise in random array imaging puts a limit on the obtainable SNR, the URA has no such limit. Computer simulations show that the URA with significant shot and background noise is vastly superior to random array techniques without noise. Implementation permits a detector which is smaller than its random array counterpart.

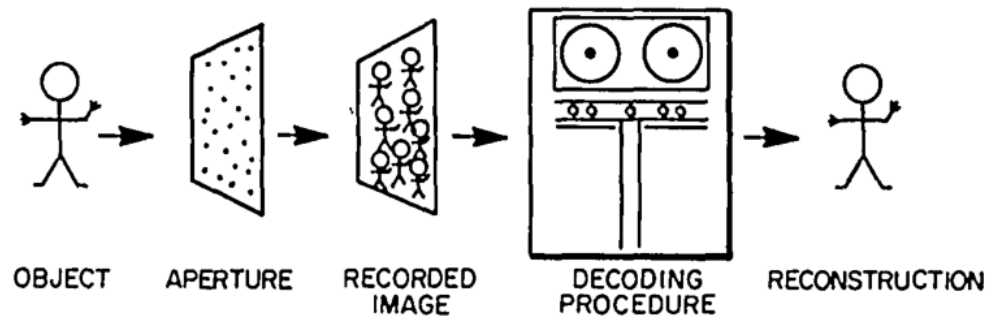


Fig. 1. The basic steps involved in coded aperture imaging are shown above. In an attempt to obtain a higher SNR, a multiple-pinhole aperture is used to form many overlapping images of the object. The resulting recorded picture must be decoded, using either a digital or optical method. The resulting reconstruction is of higher quality than that obtained by using a simple pinhole.

Coded aperture imaging with uniformly redundant arrays

E. E. Fenimore and T. M. Cannon

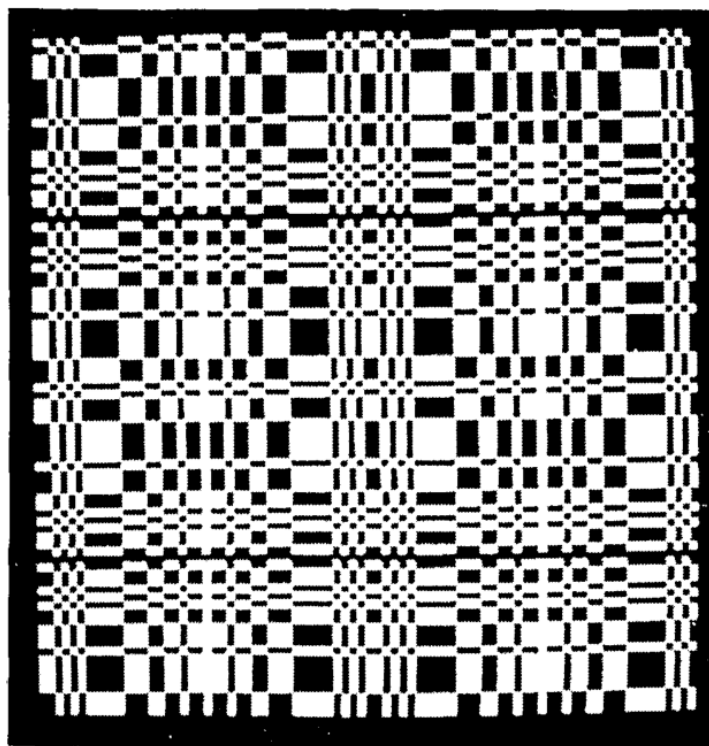
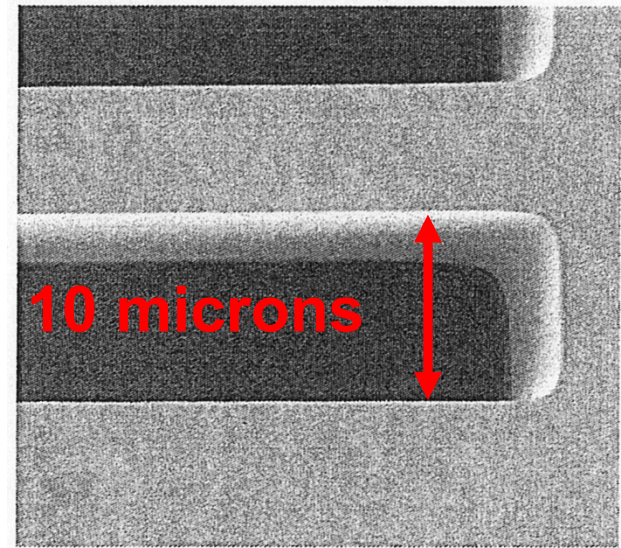
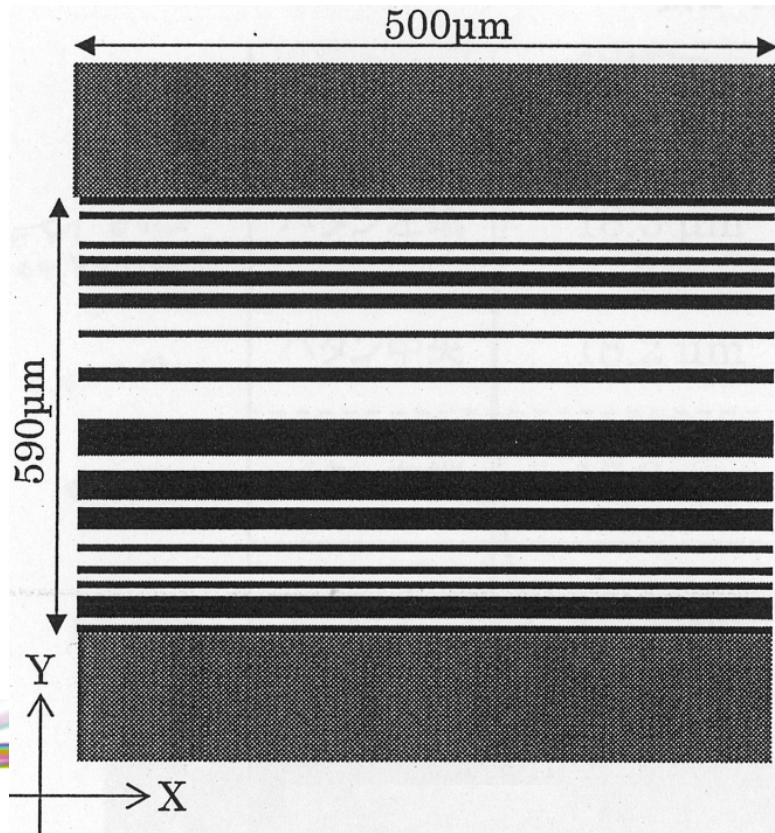


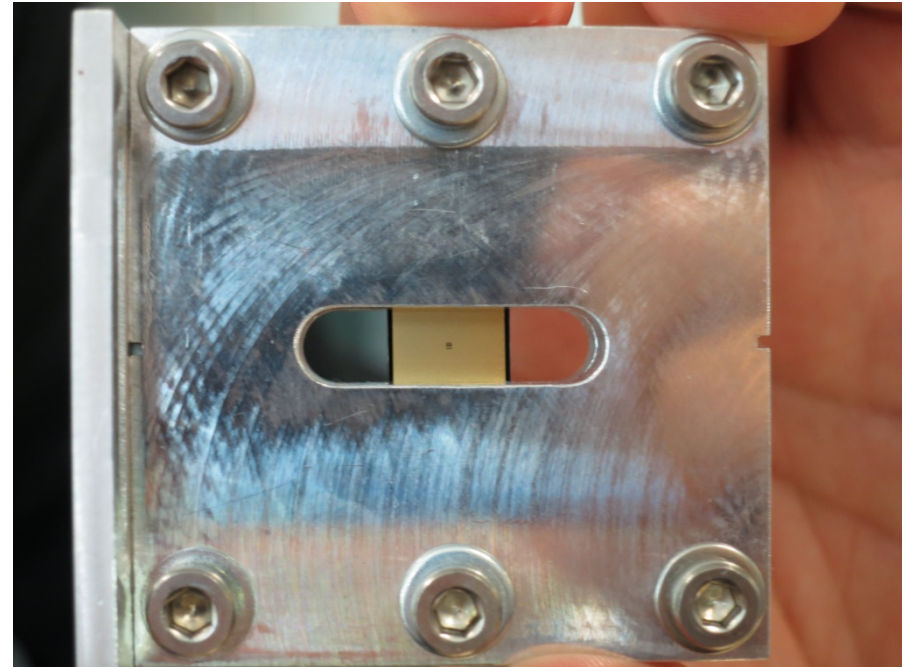
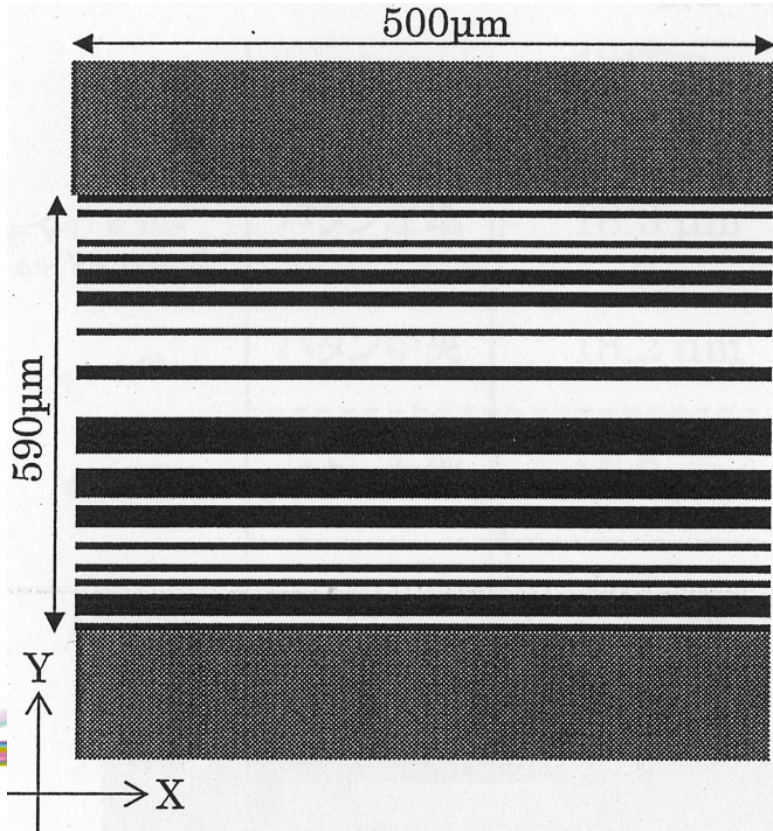
Fig. 2. A coded aperture comprised of a $2r$ by $2s$ section of a mosaic of uniformly redundant arrays each of size r by s . In this particular case $r = 43$ and $s = 41$.

The coded aperture installed at Diamond



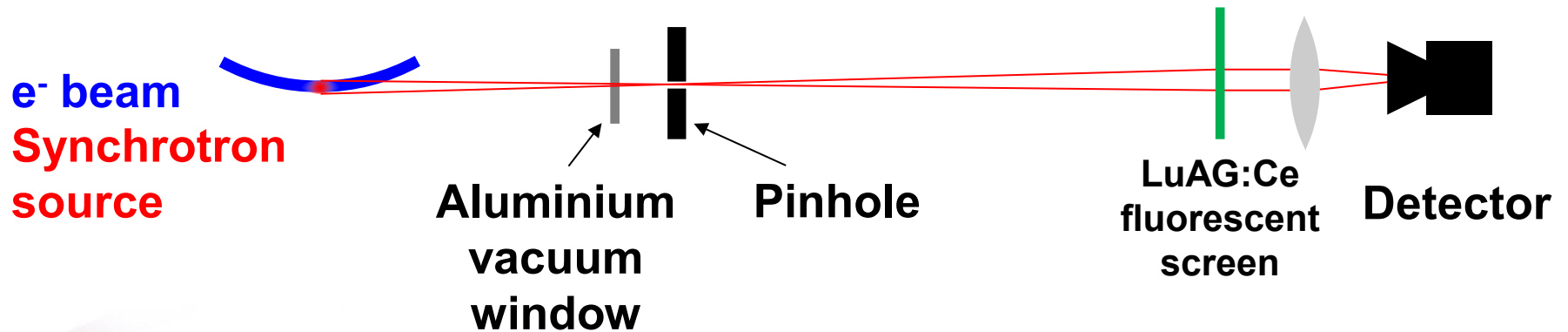
x5000 electron microscope
image of the aperture

The coded aperture installed at Diamond

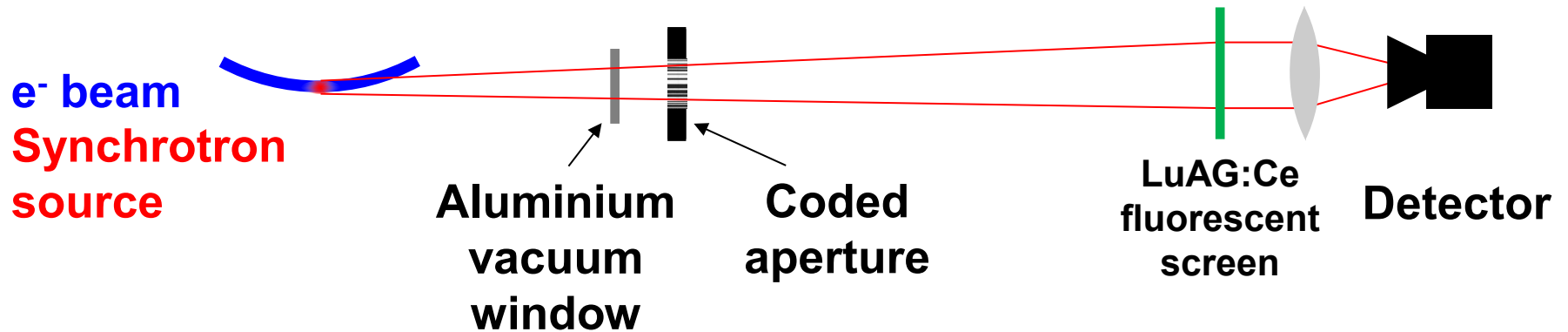


The gold coded aperture mask in an aluminium mount

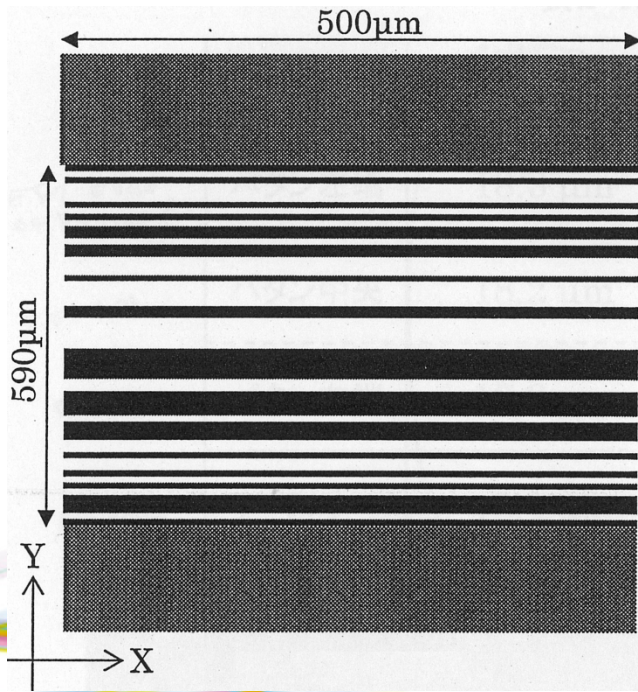
The coded aperture installed at Diamond



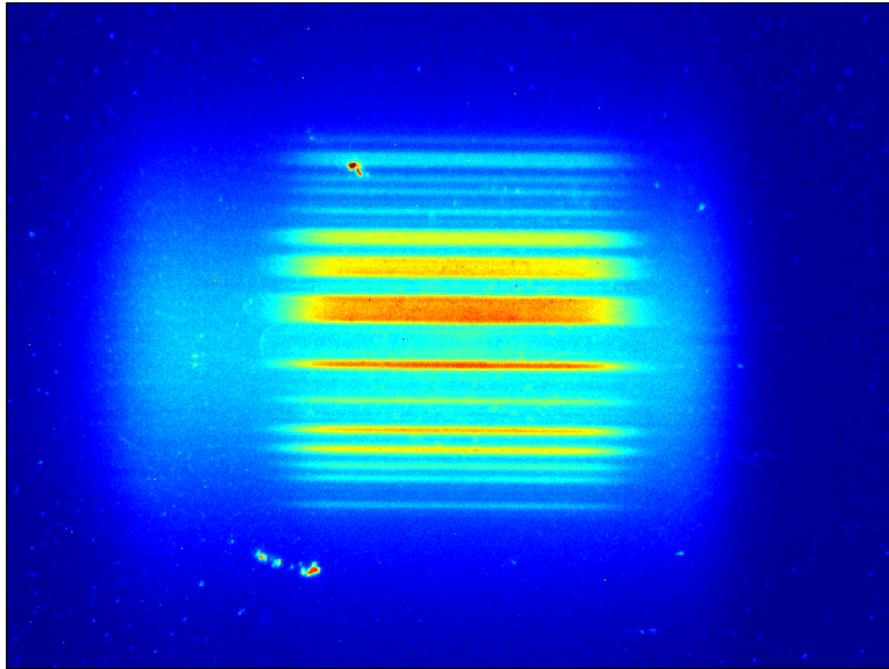
The coded aperture installed at Diamond



The coded aperture installed at Diamond

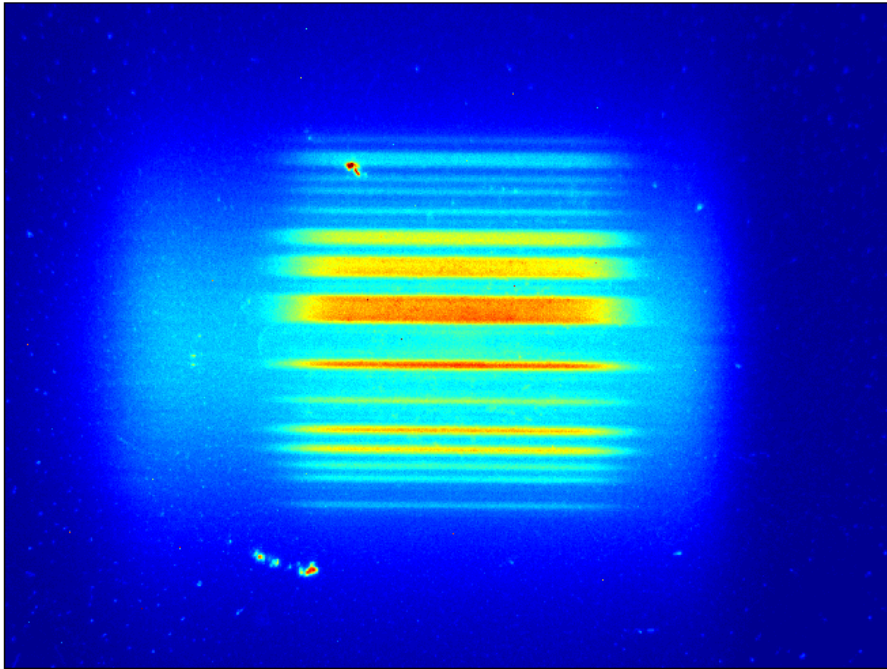


The coded aperture installed at Diamond



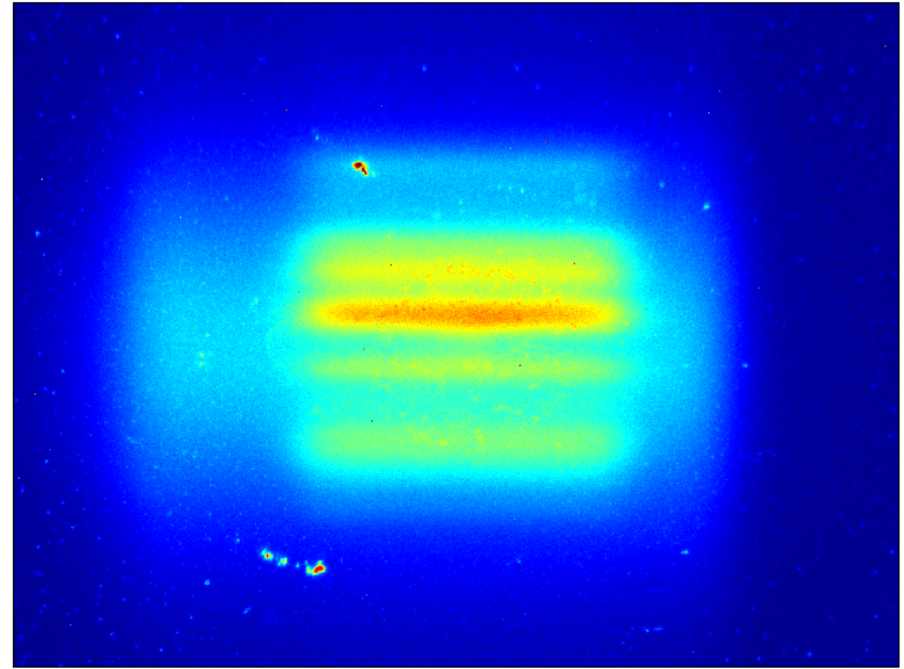
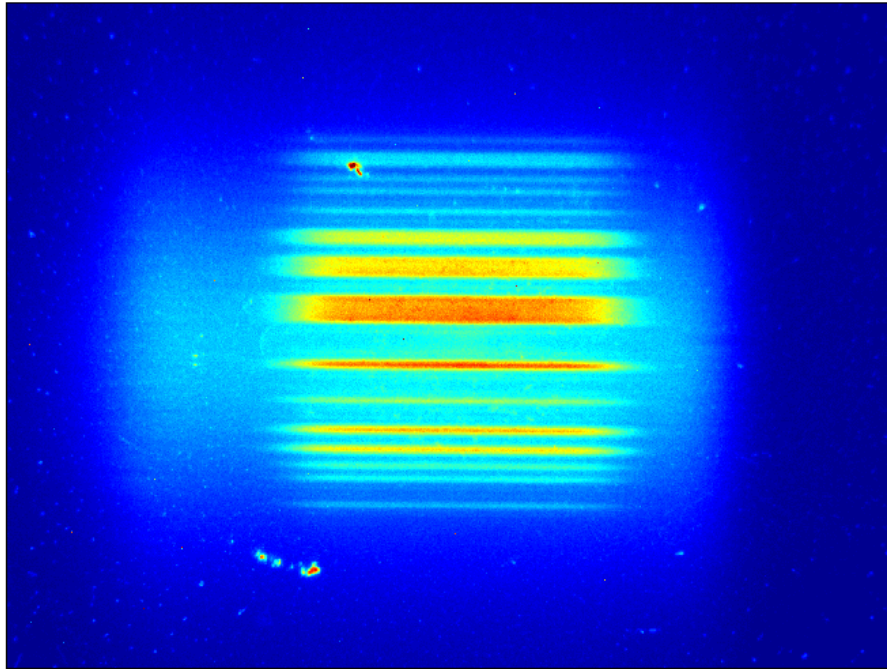
The coded aperture installed at Diamond

0.1% coupling
6 μm vertical size



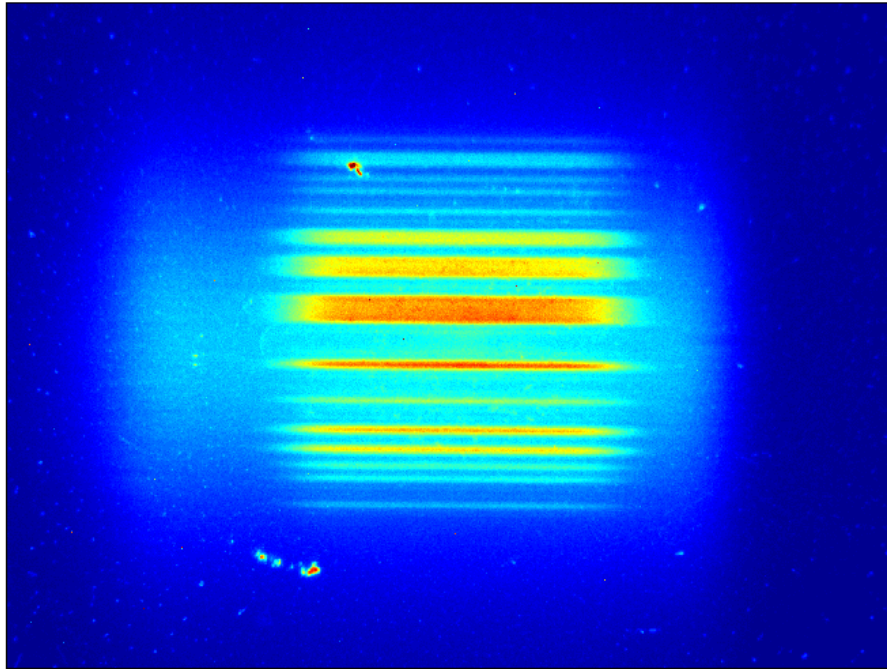
The coded aperture installed at Diamond

0.1% coupling
6 μm vertical size

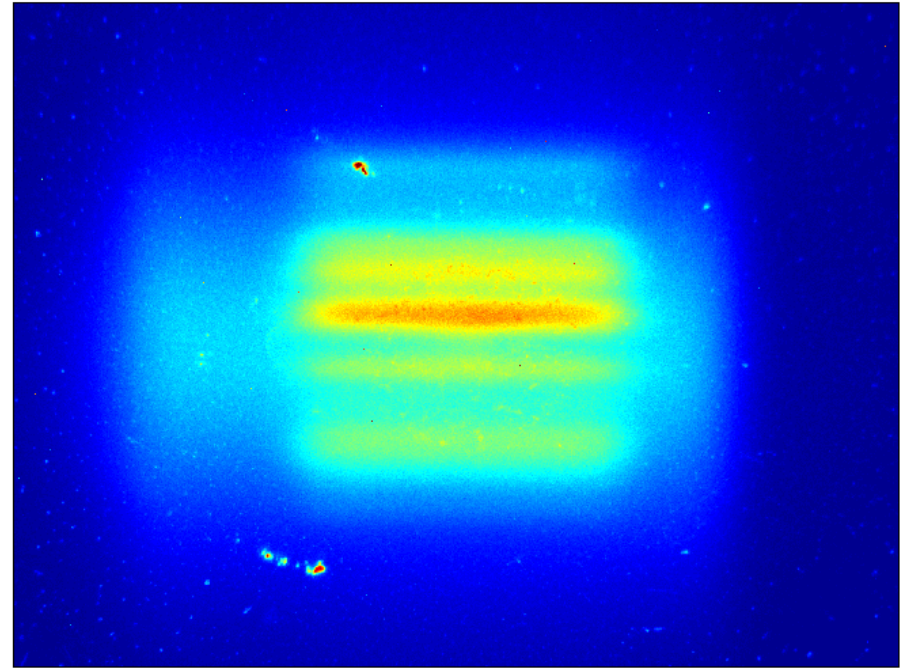


The coded aperture installed at Diamond

0.1% coupling
6 μm vertical size



1.1% coupling
26 μm vertical size

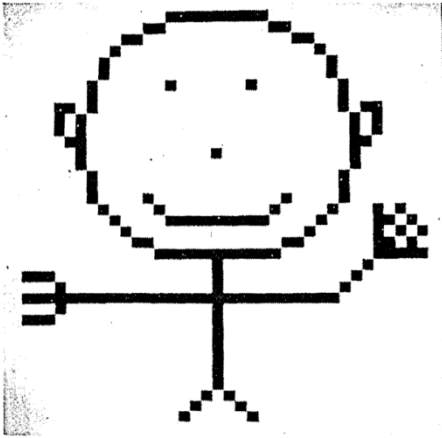


Coded aperture imaging with uniformly redundant arrays

E. E. Fenimore and T. M. Cannon

Coded aperture imaging with uniformly redundant arrays

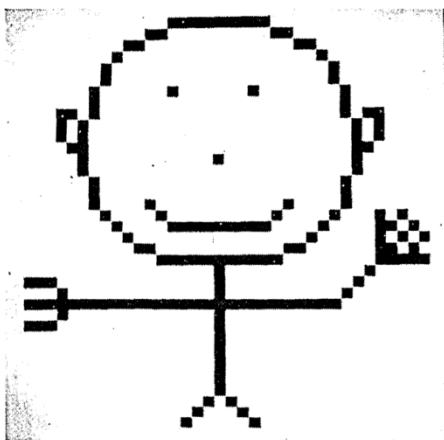
E. E. Fenimore and T. M. Cannon



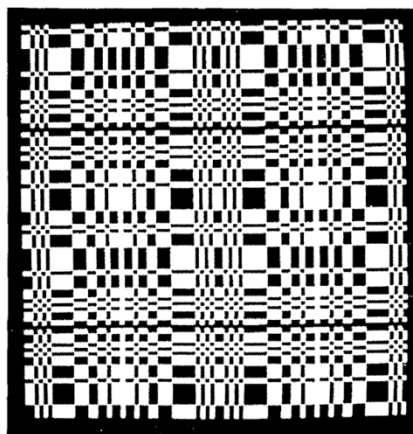
(a)

Coded aperture imaging with uniformly redundant arrays

E. E. Fenimore and T. M. Cannon

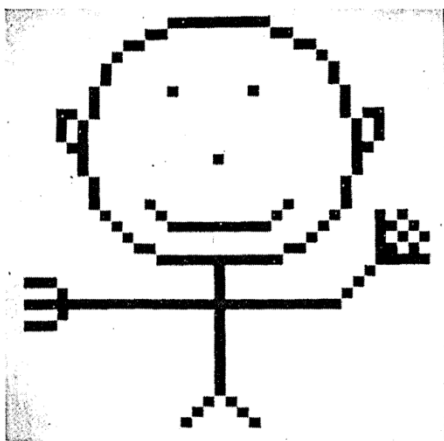


(a)

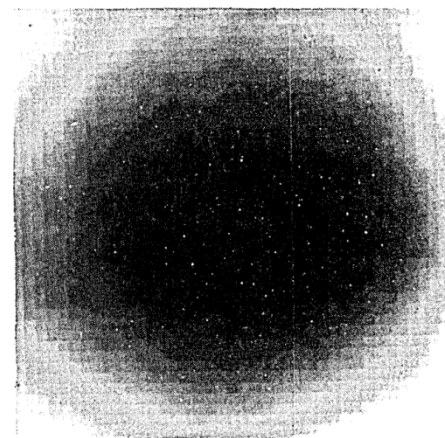
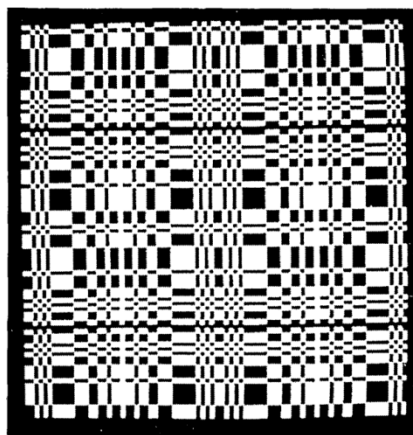


Coded aperture imaging with uniformly redundant arrays

E. E. Fenimore and T. M. Cannon

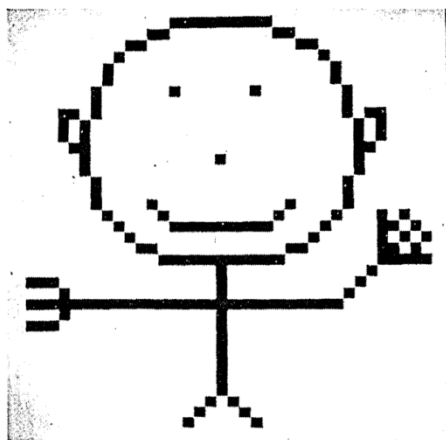


(a)

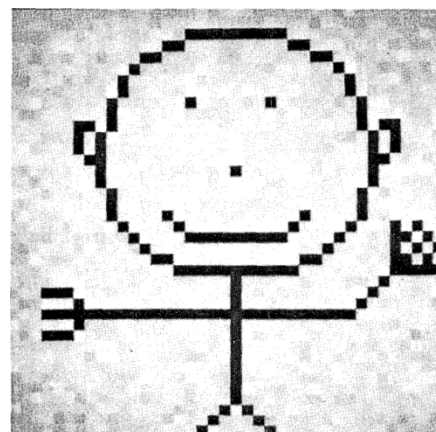
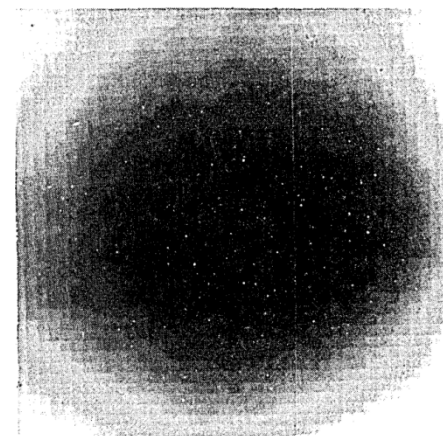
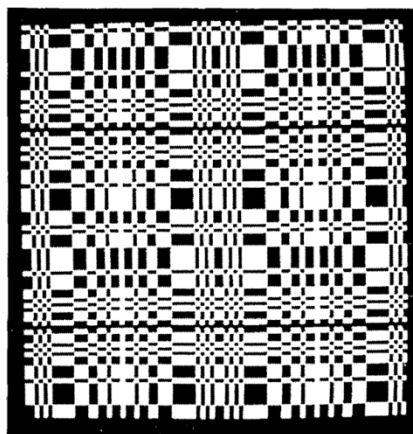


Coded aperture imaging with uniformly redundant arrays

E. E. Fenimore and T. M. Cannon

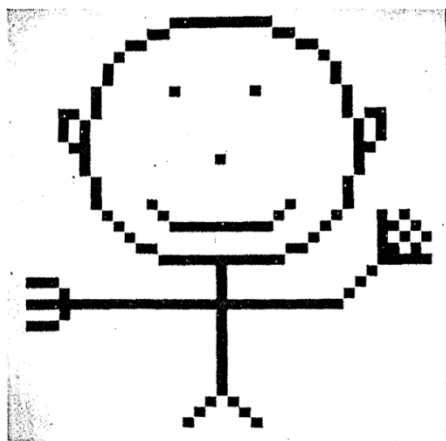


(a)

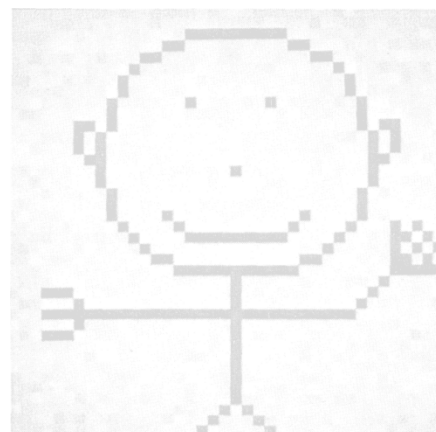
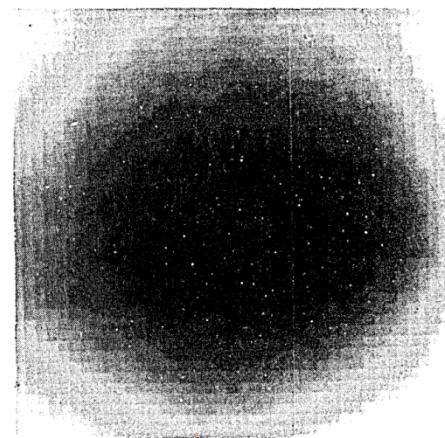
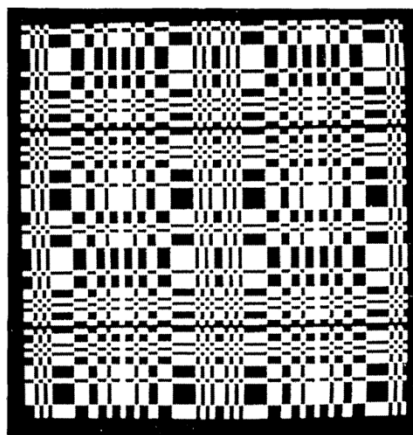


Coded aperture imaging with uniformly redundant arrays

E. E. Fenimore and T. M. Cannon

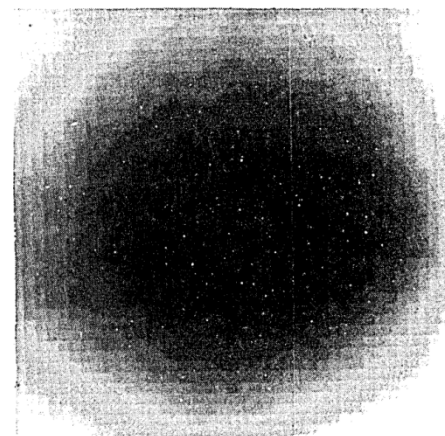
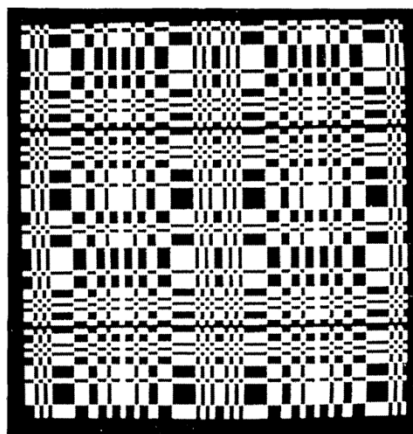
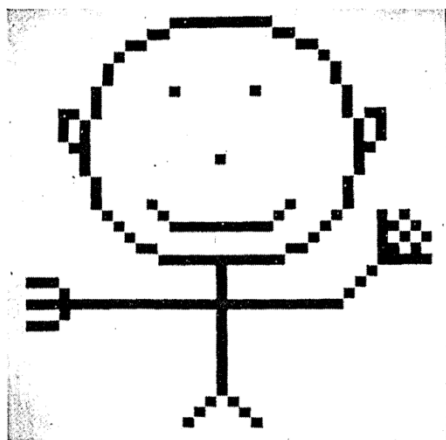


(a)



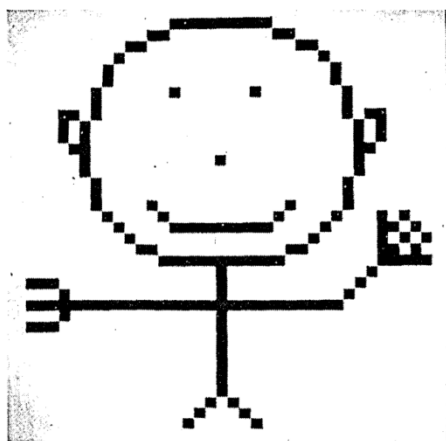
Coded aperture imaging with uniformly redundant arrays

E. E. Fenimore and T. M. Cannon

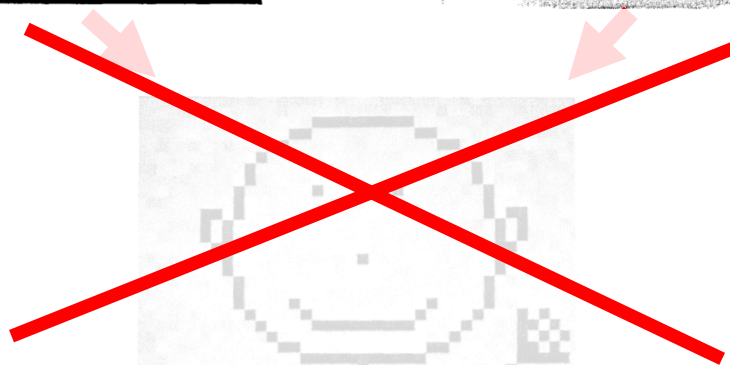
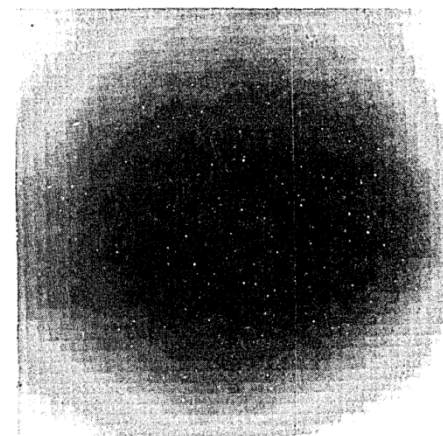
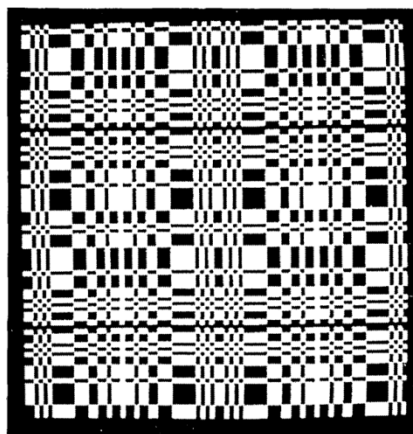


Coded aperture imaging with uniformly redundant arrays

E. E. Fenimore and T. M. Cannon



(a)



- **Scattering**
- **Noise**
- **Diffraction**
- **Non-uniform energy distribution**
- **Imprecise knowledge of our coded aperture (point spread function)**

Create templates by modelling the propagation of synchrotron radiation through the coded aperture

Proceedings of PAC09, Vancouver, BC, Canada

TH5RFP048

PERFORMANCE OF CODED APERTURE X-RAY OPTICS WITH LOW EMITTANCE BEAM AT CESRTA*

J.W. Flanagan[†], H. Fukuma, S. Hiramatsu, H. Ikeda, K. Kanazawa, T. Mitsuhashi, J. Urakawa
KEK, Tsukuba, Ibaraki 305-0801, Japan
G.S. Varner, U. Hawaii, Honolulu, HI 96822, USA
J.P. Alexander, W.H. Hopkins, B. Kreis, M.A. Palmer, D.P. Peterson,
CLASSE, Cornell U., Ithaca, NY 14853, USA

Abstract

We are working on the development of a high-speed x-ray beam profile monitor for high-resolution and fast response for beam profile measurements to be used at CEsRTA and SuperKEKB.[1] The optics for the monitor are based on coded-aperture imaging, which should permit broad-spectrum, low-distortion measurements to maximize the observable photon flux per bunch. Coupled with a high-speed digitizer system, the goal is to make turn-by-turn, bunch-by-bunch beam profile measurements. Following initial tests with a low-resolution mask at large beam sizes (vertical size $\approx 200 \mu\text{m}$), a high-resolution mask has been made for use with low-emittance beams (vertical size $\approx 10 \mu\text{m}$) at CEsrTA. We discuss the methods for analyzing the coded aperture mask data, and some preliminary performance results of the use of the high-resolution mask on the low-emittance CEsrTA beam in January 2009.

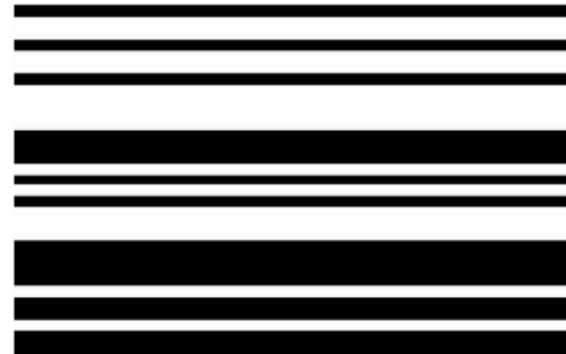


Figure 1: Coded aperture test mask used in January 2009 beam test at CEsrTA. (Aspect ratio not to scale.)

Create templates by modelling the propagation of synchrotron radiation through the coded aperture

Proceedings of PAC09, Vancouver, BC, Canada

TH5RFP048

PERFORMANCE OF CODED APERTURE X-RAY OPTICS WITH LOW EMITTANCE BEAM AT CESRTA*

J.W. Flanagan[†], H. Fukuma, S. Hiramatsu, H. Ikeda, K. Kanazawa, T. Mitsuhashi, J. Urakawa
KEK, Tsukuba, Ibaraki 305-0801, Japan
G.S. Varner, U. Hawaii, Honolulu, HI 96822, USA
J.P. Alexander, W.H. Hopkins, B. Kreis, M.A. Palmer, D.P. Peterson,
CLASSE, Cornell U., Ithaca, NY 14853, USA

Simulation Method

Following K.J. Kim's formulation[6], the σ and π components of the complex wavefront amplitude of the component of synchrotron radiation (SR) with angular frequency ω can be written as

$$\begin{bmatrix} A_\sigma \\ A_\pi \end{bmatrix} = \frac{\sqrt{3}}{2\pi} \gamma \frac{\omega}{\omega_c} (1 + X^2) (-i) \begin{bmatrix} K_{2/3}(\eta) \\ \frac{iX}{\sqrt{1+X^2}} K_{1/3}(\eta) \end{bmatrix},$$

CHARACTERISTICS OF SYNCHROTRON RADIATION

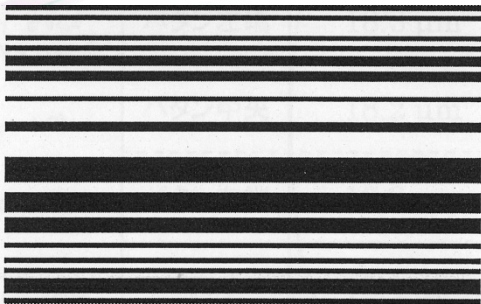
Kwang-Je Kim
Center for X-ray Optics
Accelerator and Fusion Research Division
Lawrence Berkeley Laboratory, Berkeley, CA 94720

Create templates by modelling the propagation of synchrotron radiation through the coded aperture

Parameter values

Beam size = [1, 2, 3, ..., 9, 10]
Beam position = [-5, -4, -3, ..., 4, 5]
Beam skew =
.....

Coded aperture

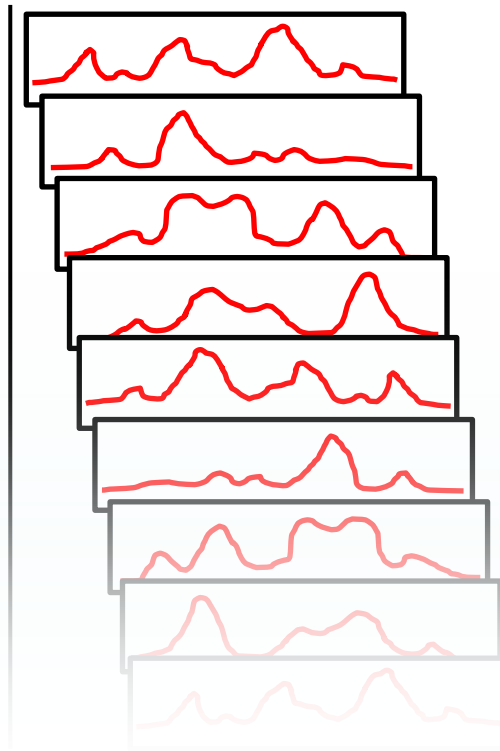


Create templates by modelling the propagation of synchrotron radiation through the coded aperture

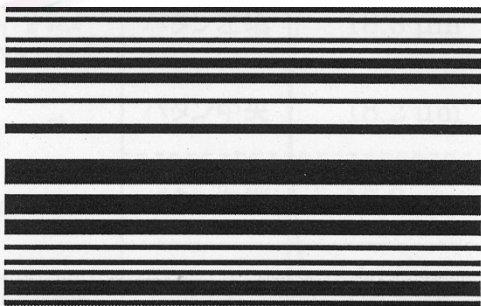
Parameter values

Beam size = [1, 2, 3, ..., 9, 10]
Beam position = [-5, -4, -3, ..., 4, 5]
Beam skew =
.....

1-dimensional templates

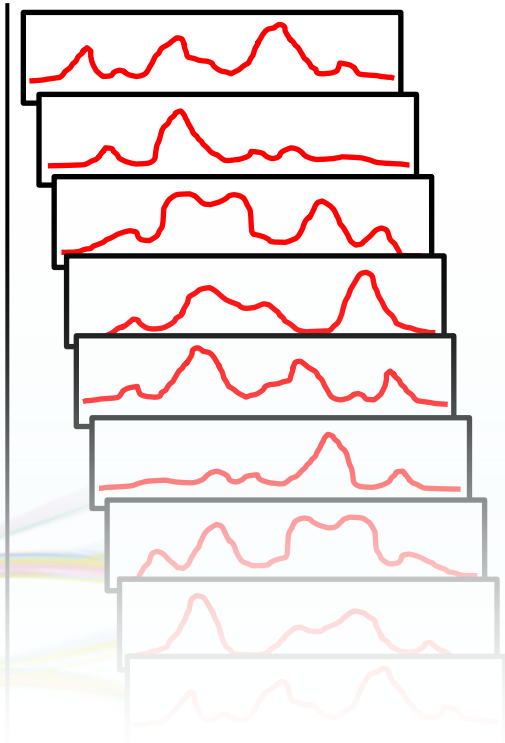


Coded aperture



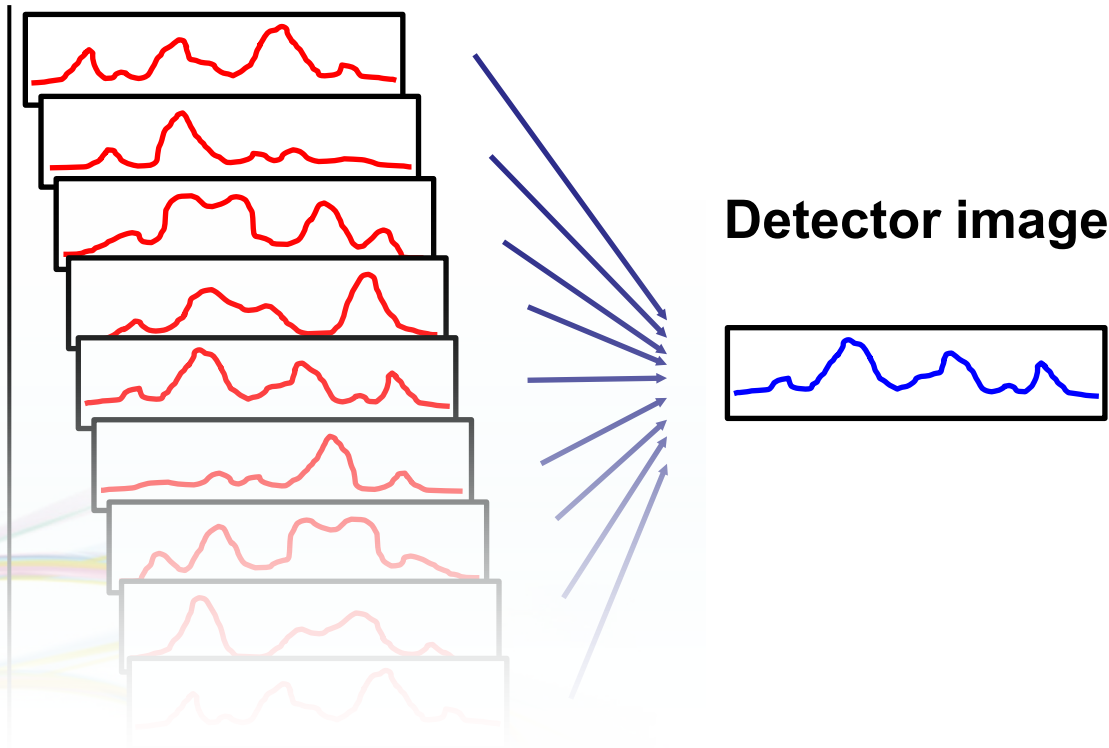
Compare the coded image from the detector with each of the templates and find the best fit

1-dimensional templates



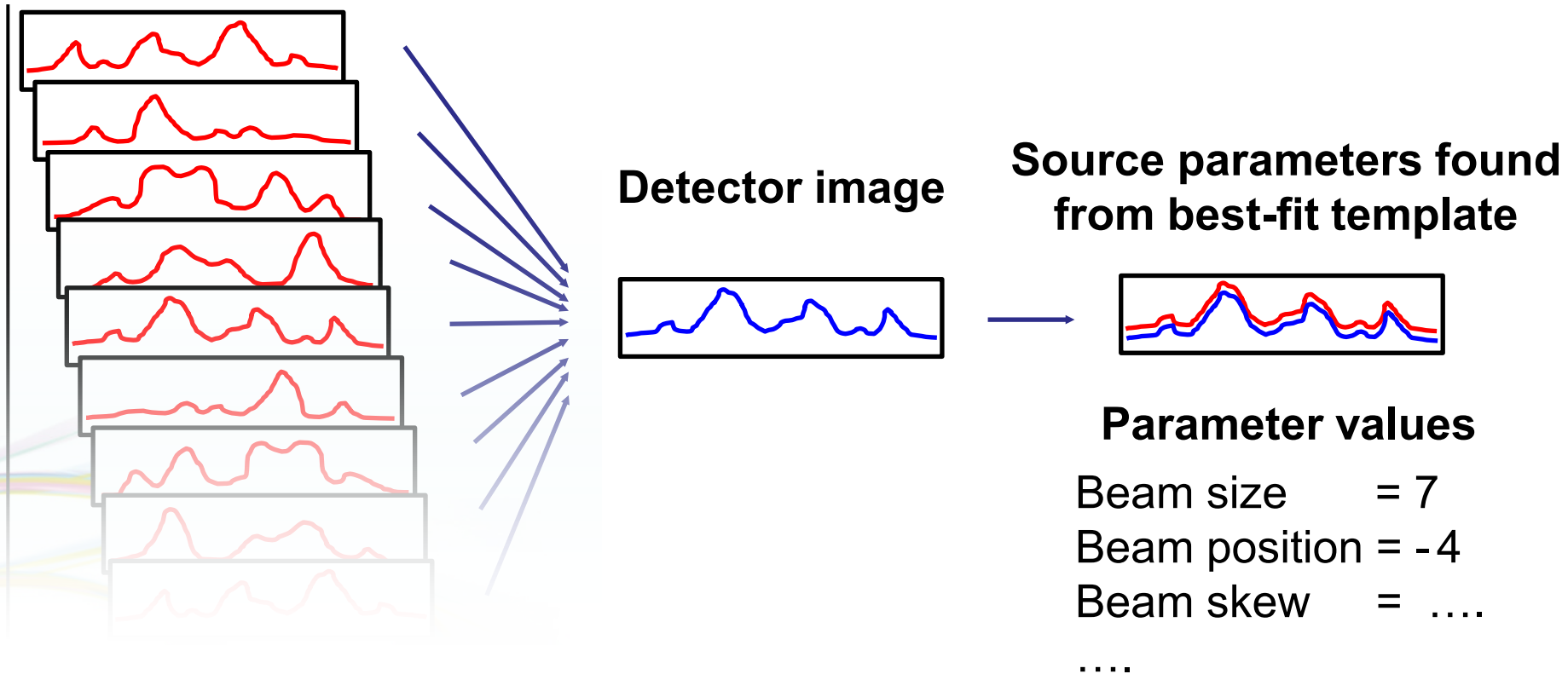
Compare the coded image from the detector with each of the templates and find the best fit

1-dimensional templates

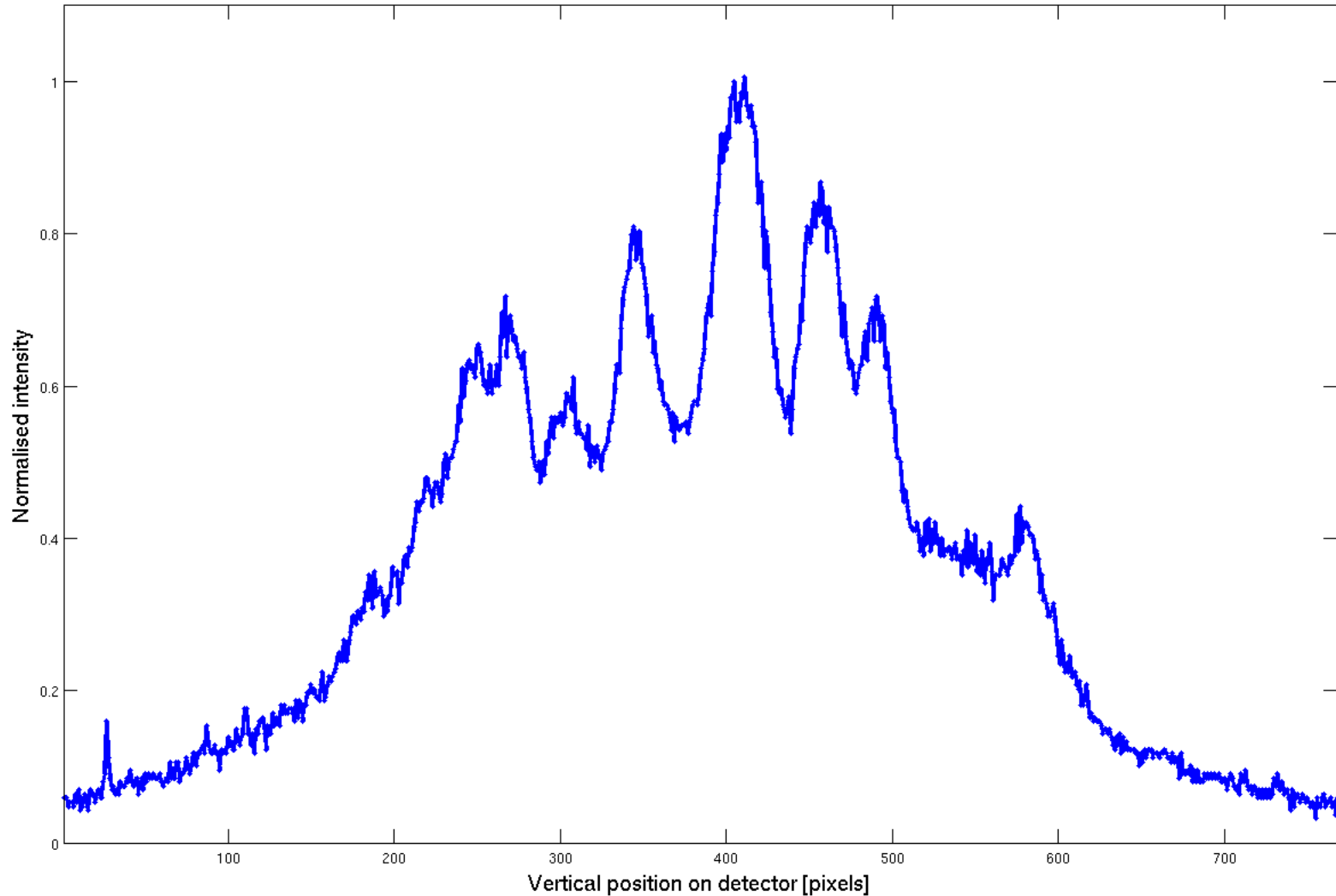


Compare the coded image from the detector with each of the templates and find the best fit

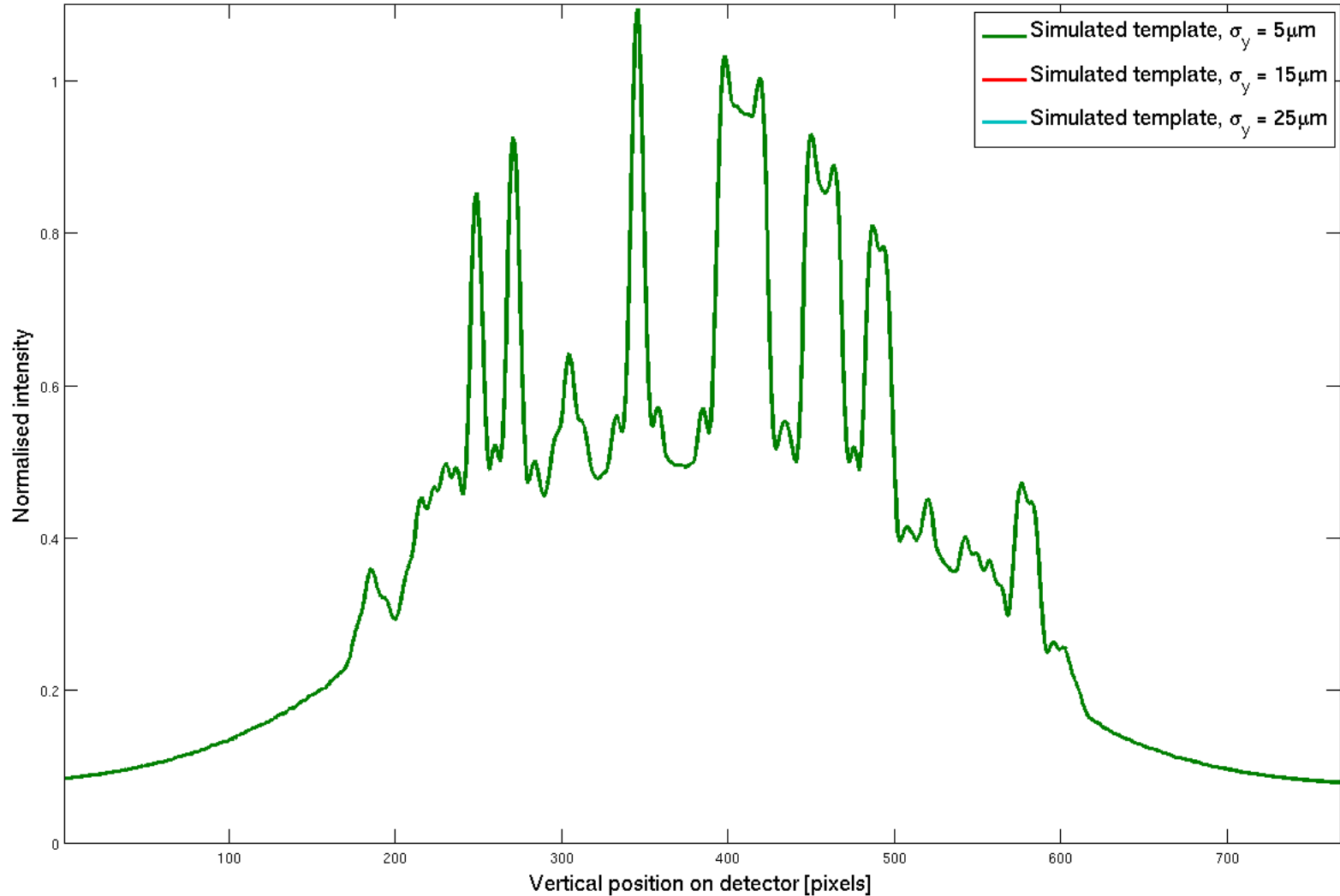
1-dimensional templates



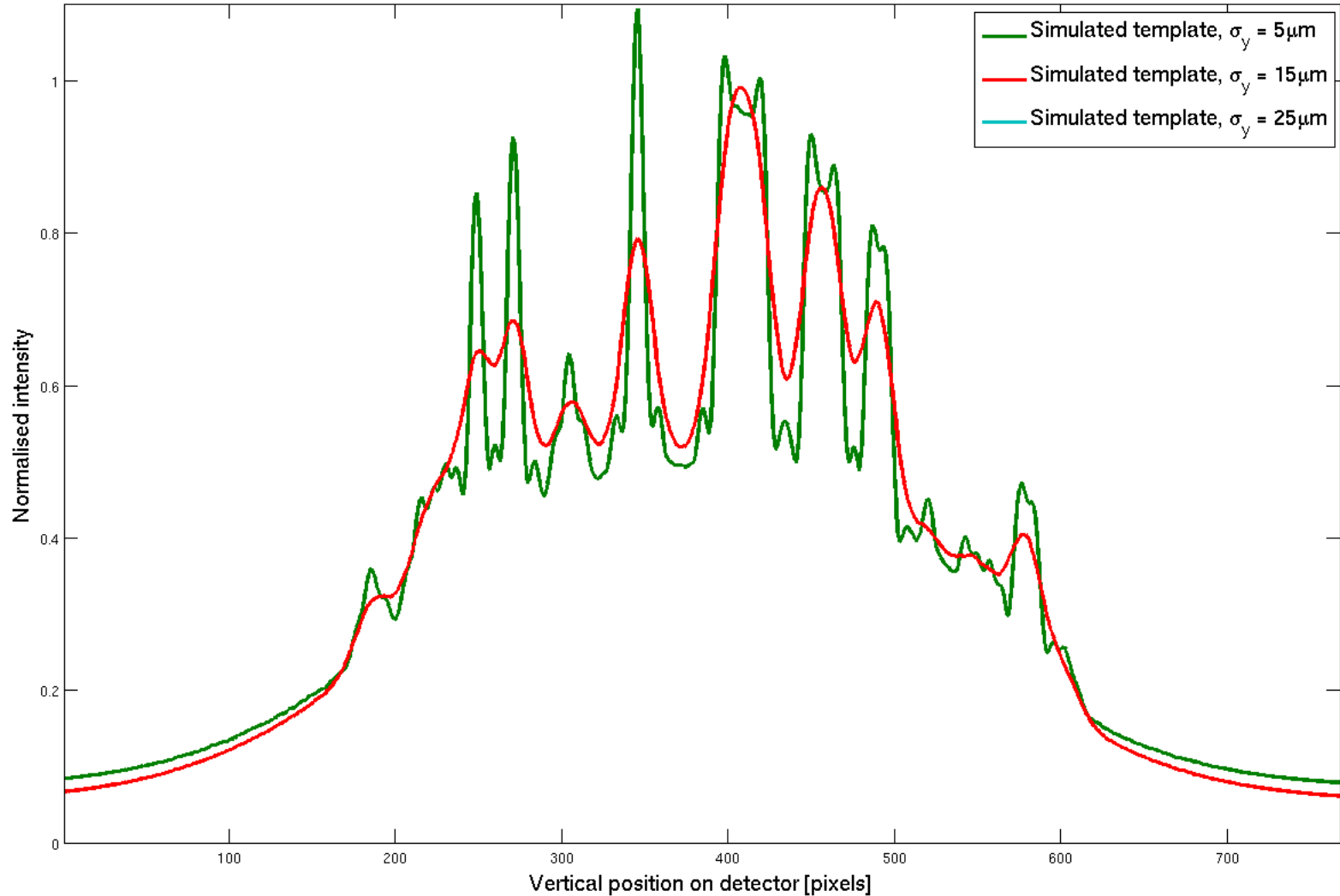
Compare the coded image from the detector with each of the templates and find the best fit



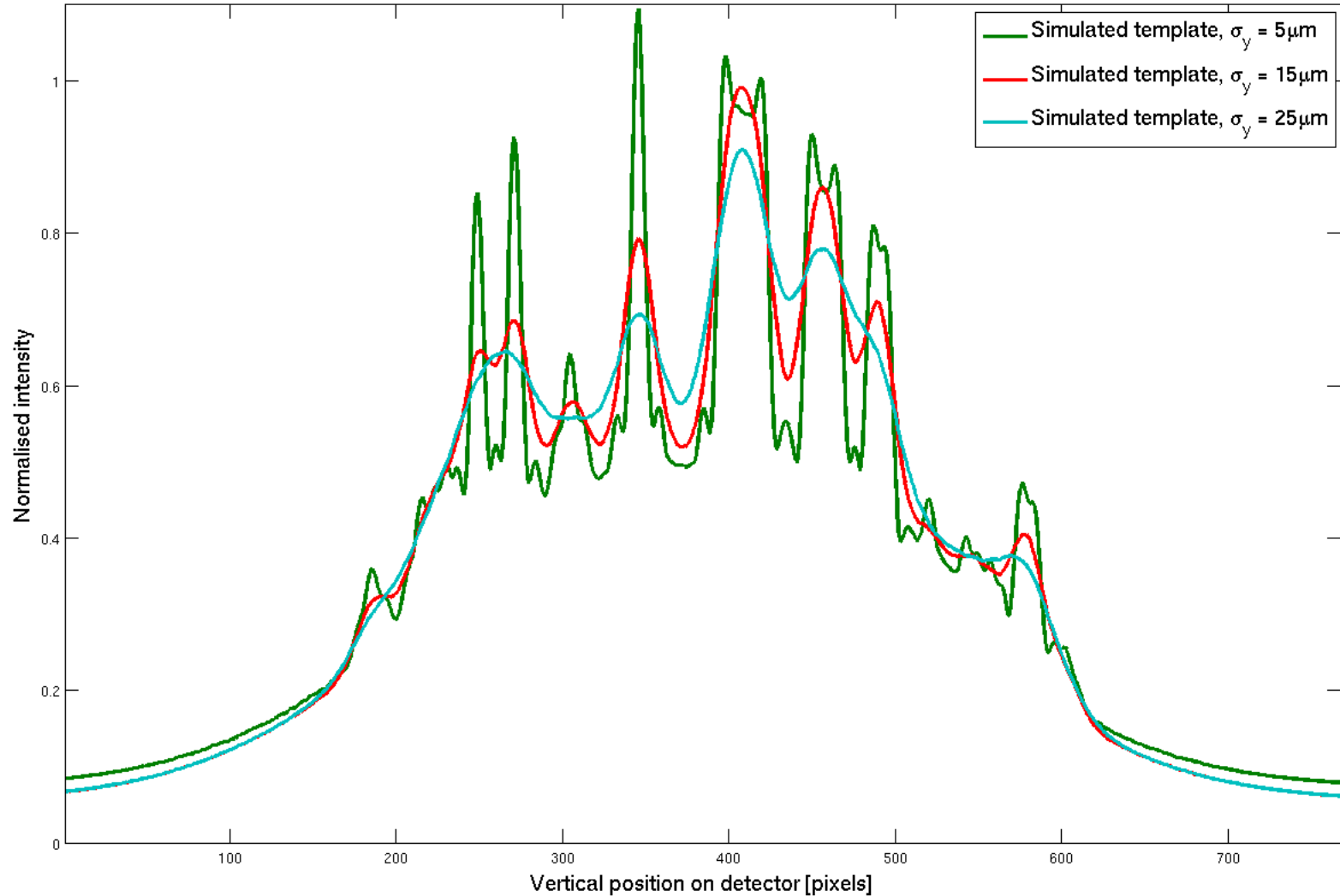
Compare the coded image from the detector with each of the templates and find the best fit



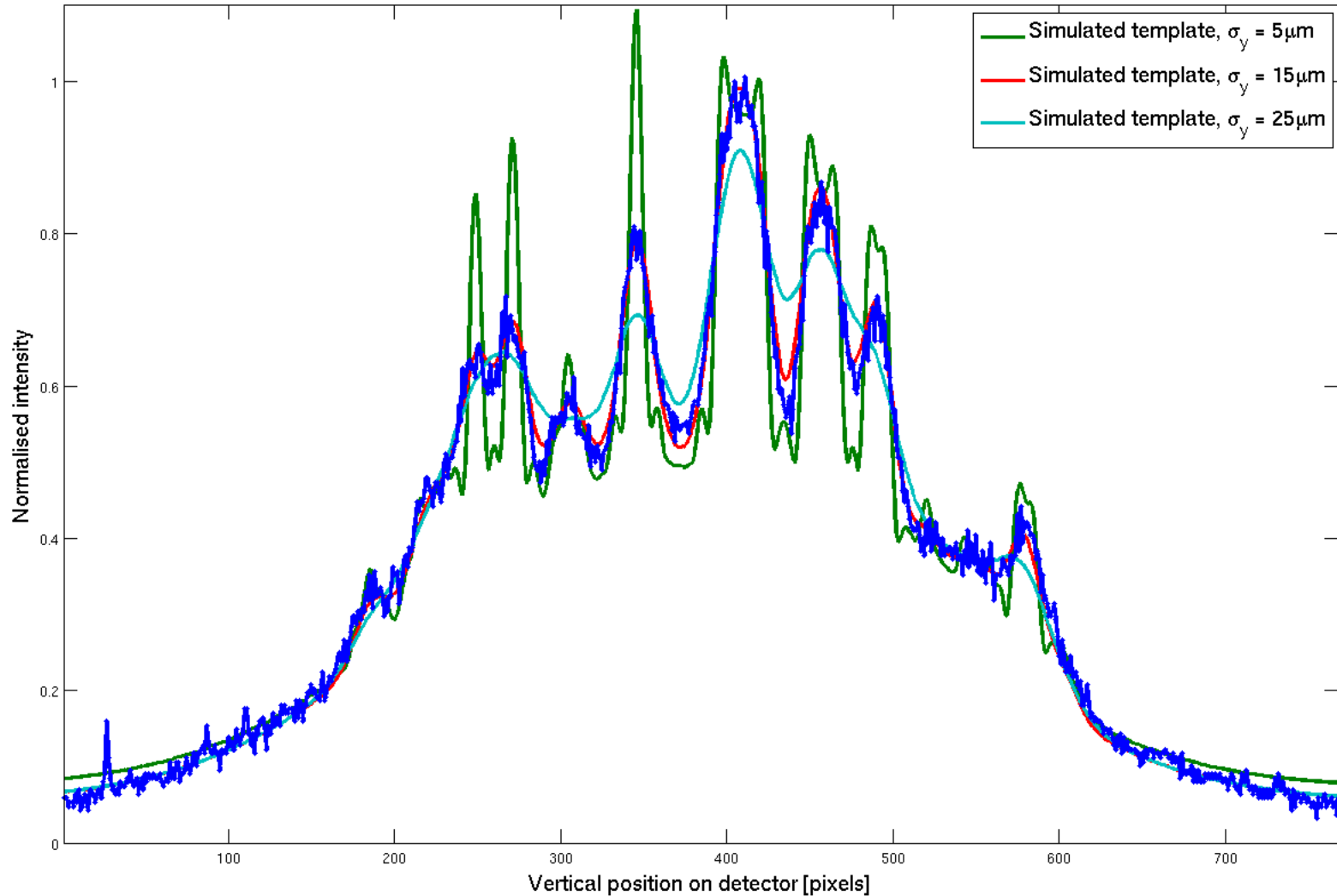
Compare the coded image from the detector with each of the templates and find the best fit



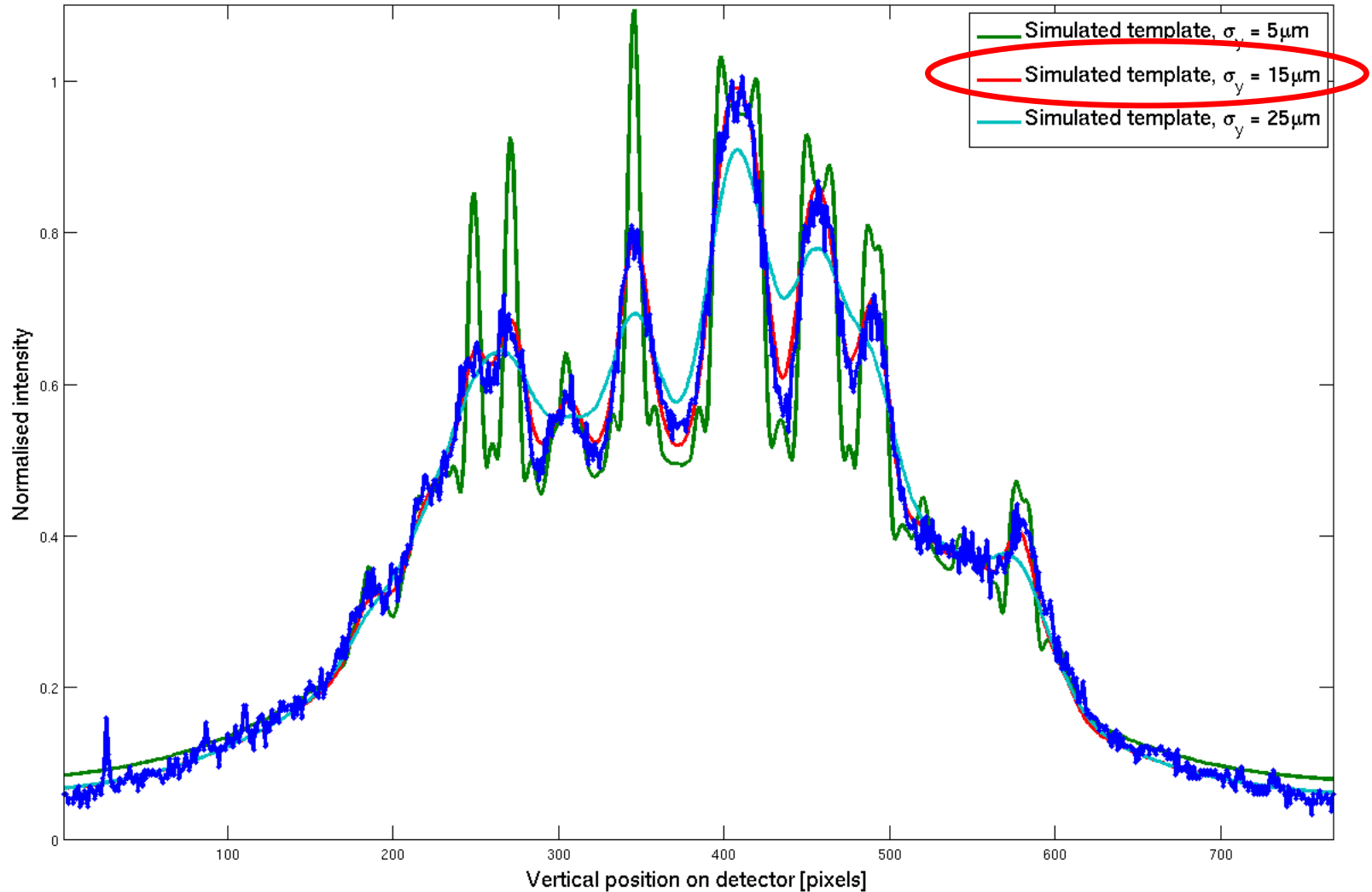
Compare the coded image from the detector with each of the templates and find the best fit

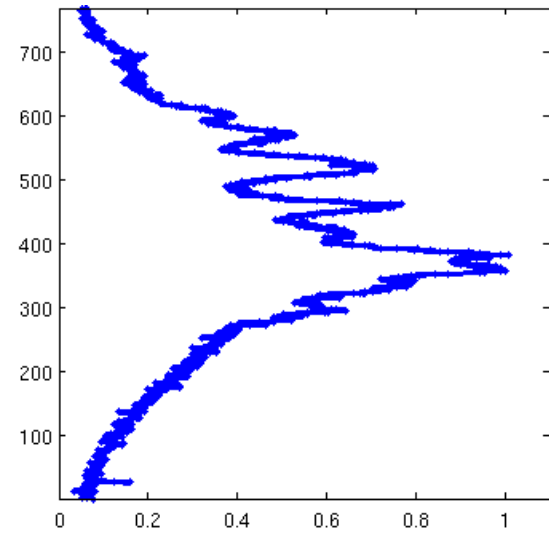
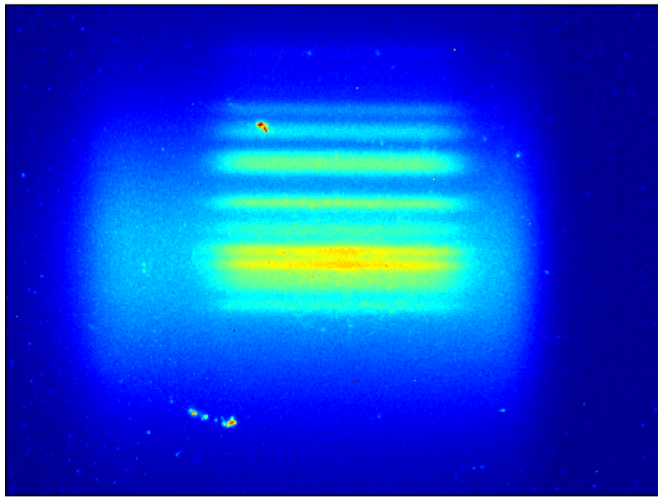


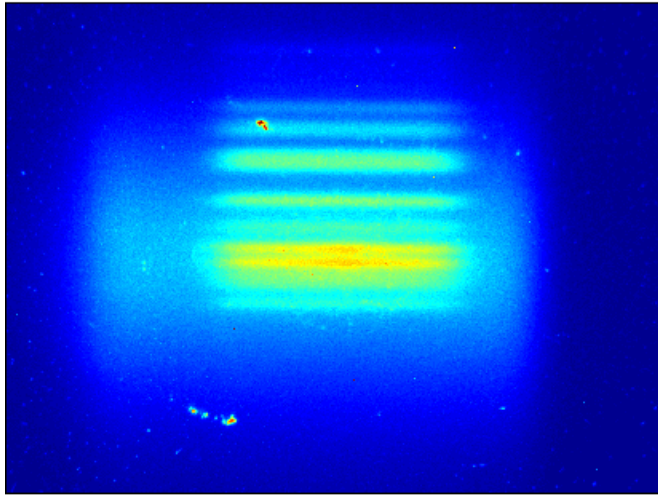
Compare the coded image from the detector with each of the templates and find the best fit



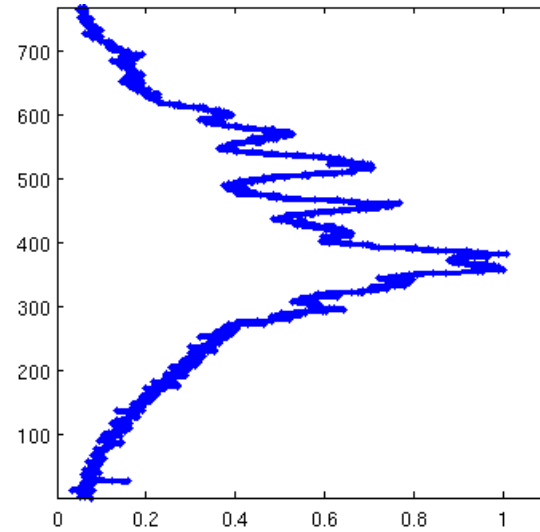
Compare the coded image from the detector with each of the templates and find the best fit

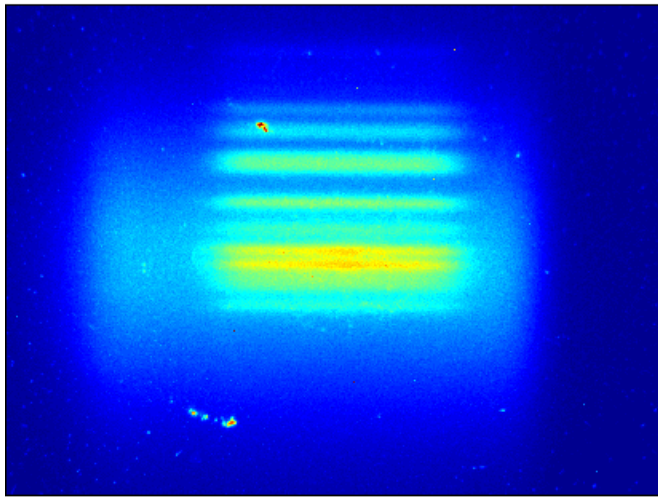




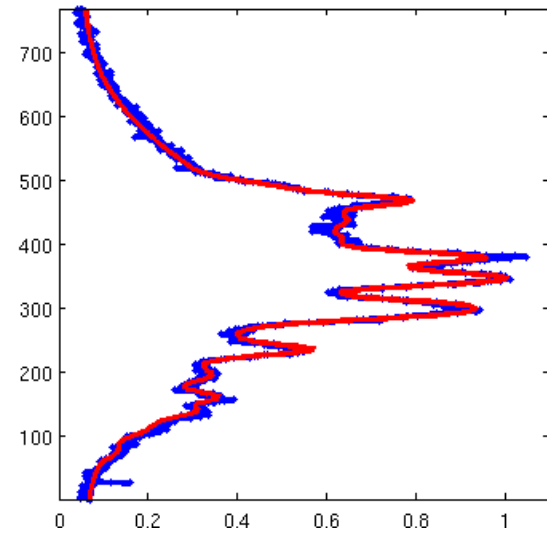
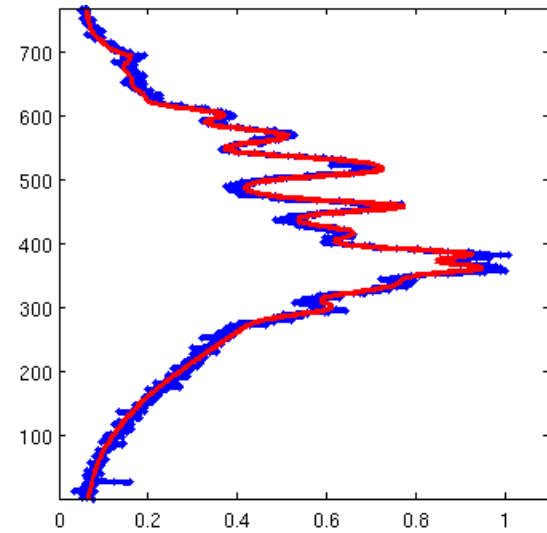
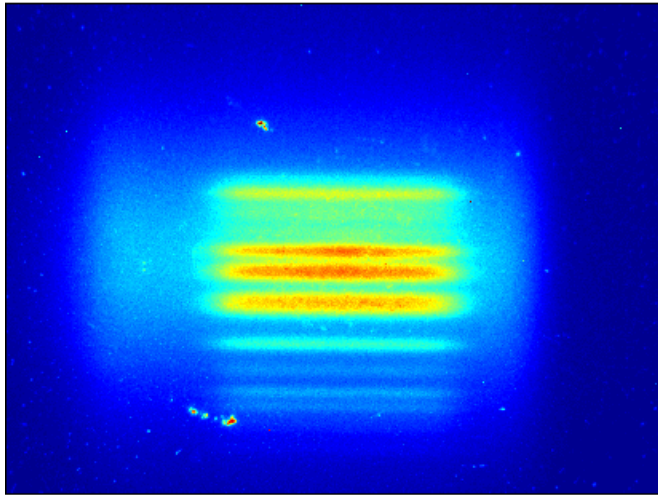


↓
300 μ m
stepper motor
movement

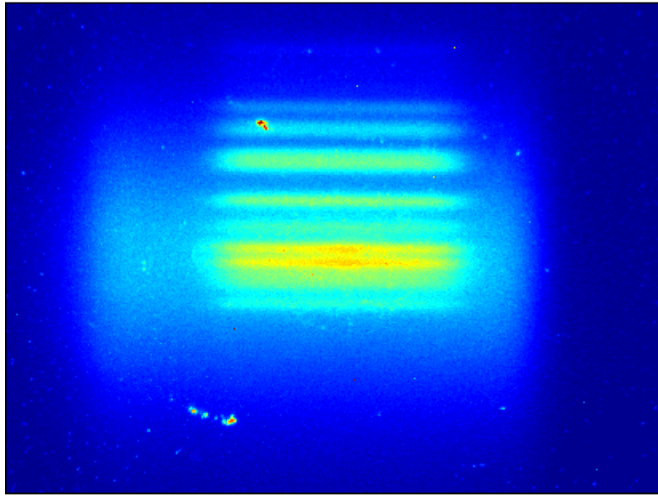




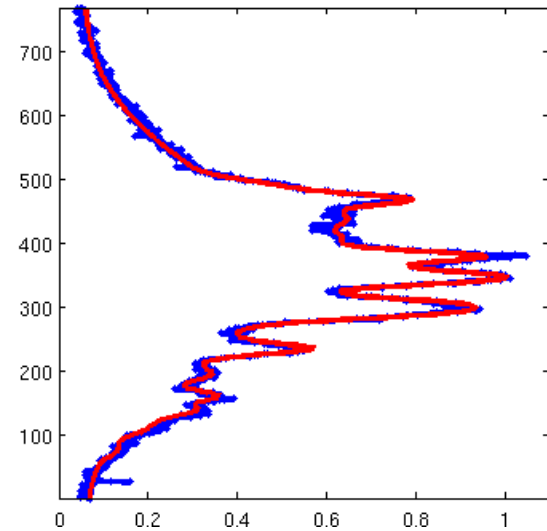
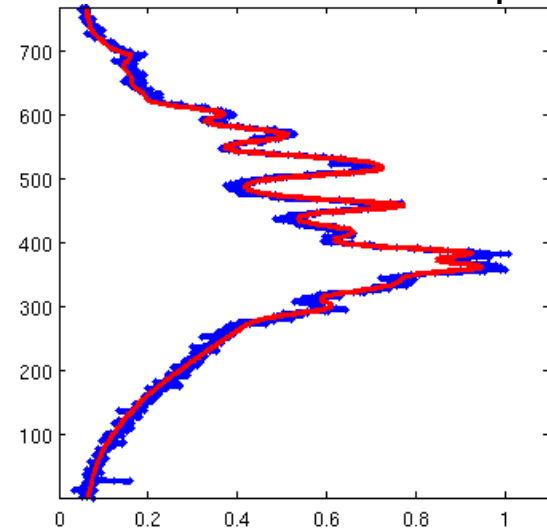
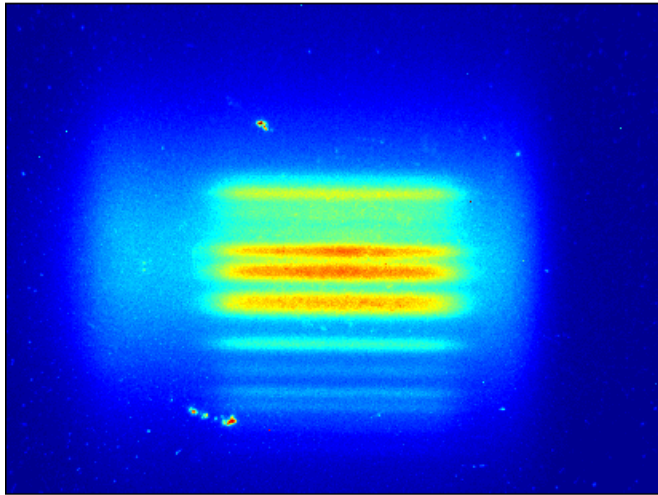
300 μ m
stepper motor
movement



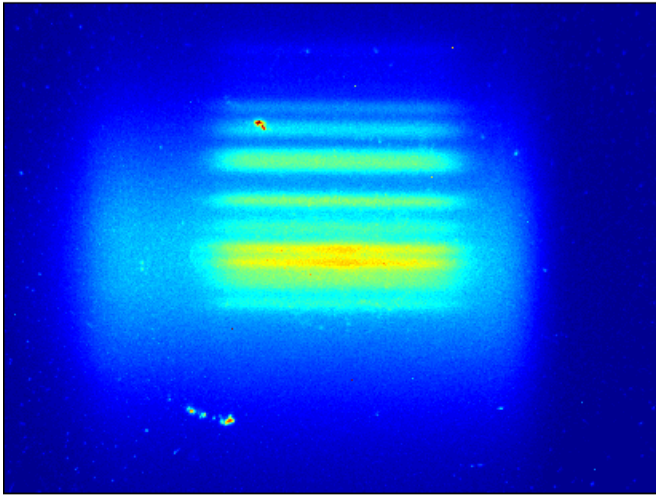
e-beam size, $\sigma_y = 14\mu\text{m}$
V. offset = $184\mu\text{m}$



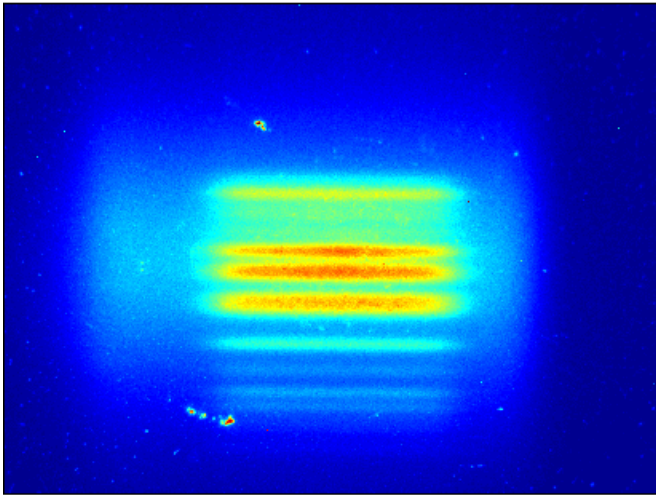
300 μm
stepper motor
movement



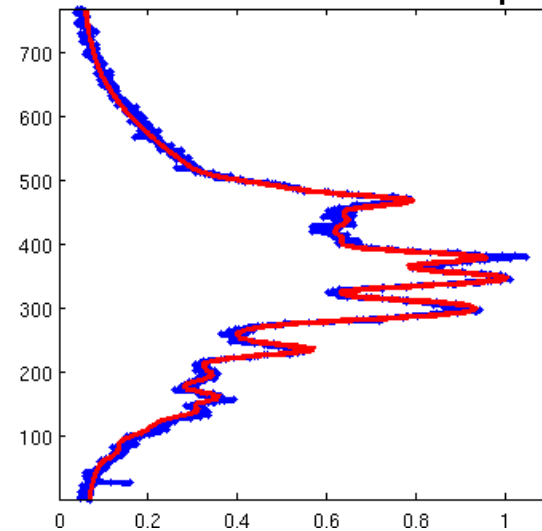
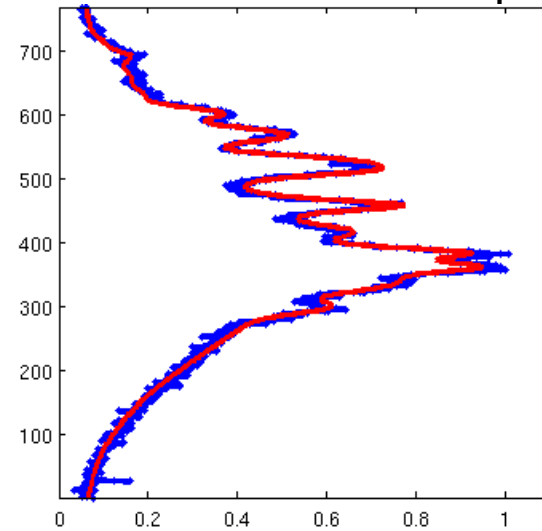
e-beam size, $\sigma_y = 14\mu\text{m}$
V. offset = $184\mu\text{m}$

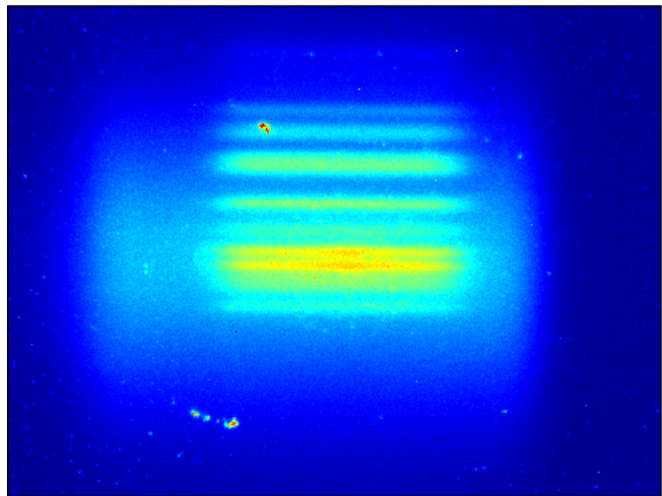


300 μm
stepper motor
movement

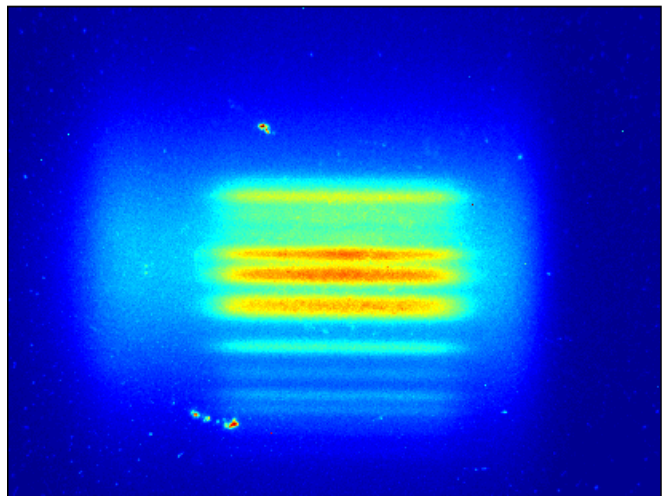


e-beam size, $\sigma_y = 14\mu\text{m}$
V. offset = $-108\mu\text{m}$

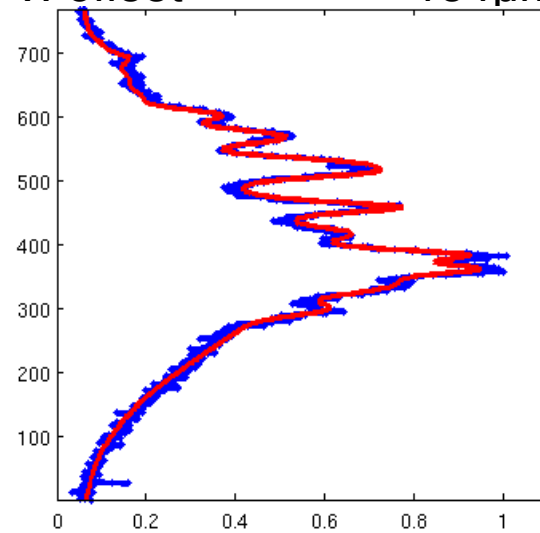




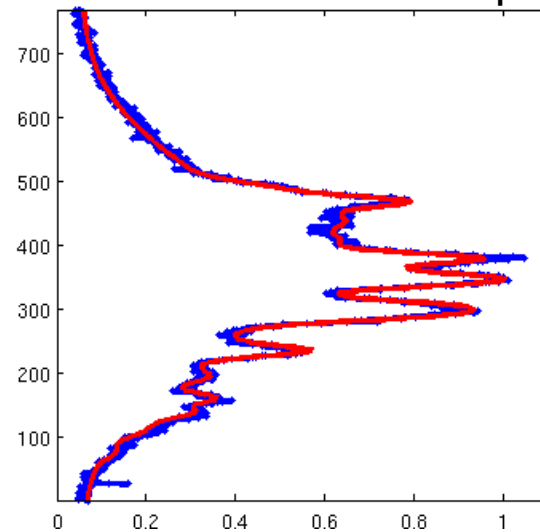
300µm
stepper motor
movement



e-beam size, $\sigma_y = 14\mu\text{m}$
V. offset = 184µm

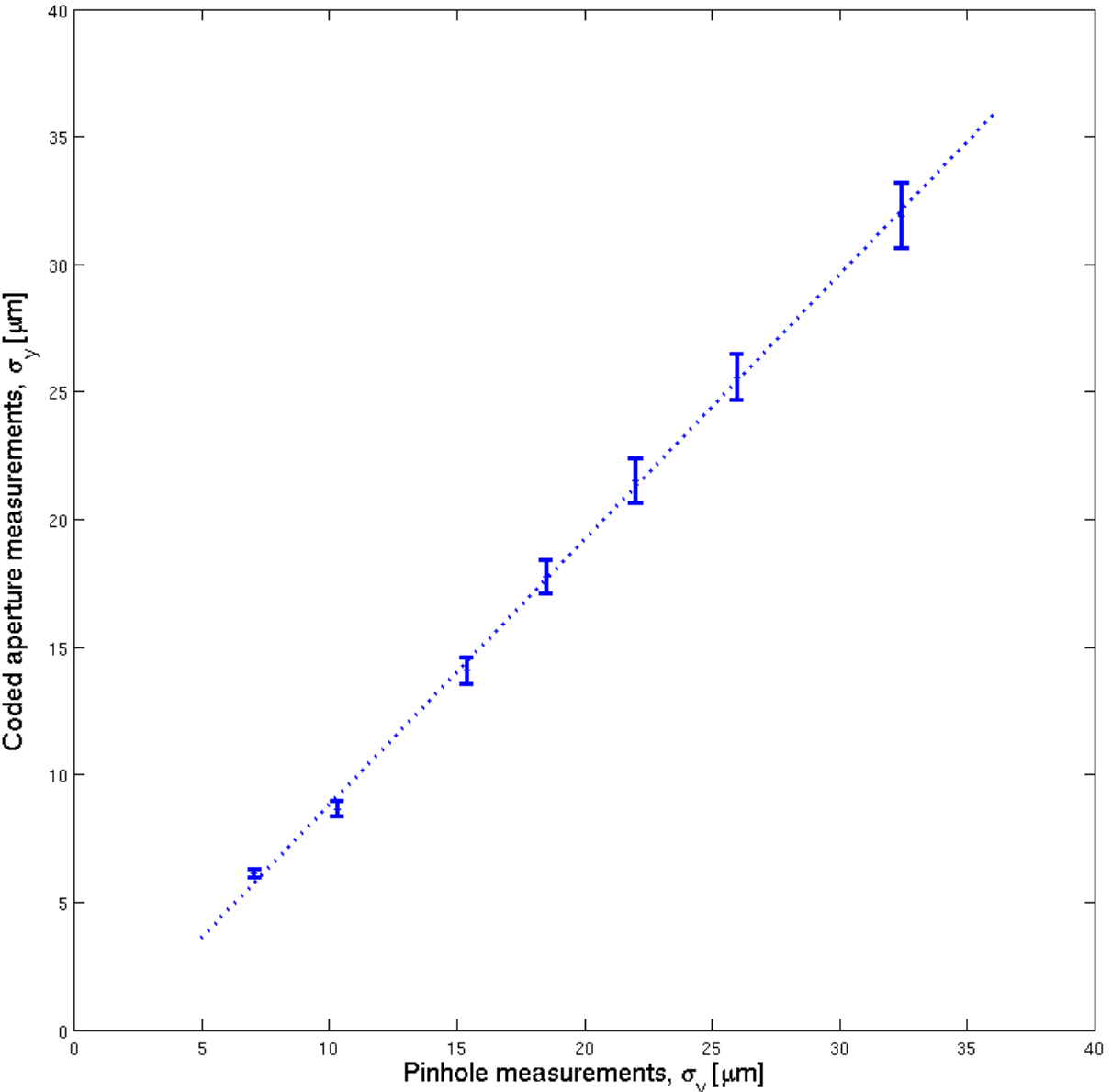


e-beam size, $\sigma_y = 14\mu\text{m}$
V. offset = -108µm



Diff. =
292µm

Comparison of coded aperture measurements with pinhole measurements



Conclusions

A coded aperture has been installed at Diamond and successfully used to make measurements of the electron beam!

Coded aperture measurements correlate well with pinhole measurements.

Smaller beam sizes seem to give us better resolution with the system.

If we want turn-by-turn measurements we need to invest in a faster detector.

Acknowledgements

John Flanagan, KEK
Guenther Rehm, Diamond
Ian Martin, Diamond